Project Number: 52

# Design, Analysis, Manufacturing, and Testing of an Electric Formula SAE Racecar

A Major Qualifying Project Report

Submitted to the Faculty

of the

WORCESTER POLYTECHNIC INSTITUTE

in partial fulfillment of the requirements for the

Degree of Bachelor of Science

in Mechanical Engineering Electrical and Computer Engineering, Robotics Engineering, and Computer Science

by

Hussain Bhatti (ECE), Harris Brancazio (ME), Henrique Checcucci (ME),
John Demedeiros (ECE), Emma Dimmig (RBE), Connor Dowgielewicz (ME),
Zoe Goodman (ECE), Carson Graham (CS), William Gunn (ME), Samuel Kierstead (ME),
Evelyn Maude (RBE), & Arnav Sacheti (CS/ECE)

Date: April 25th, 2024

Approved:

_____

Prof. William Michalson, Major Advisor

_____

Prof. David Planchard, Co-Advisor

_____

Prof. Andre Rosendo, Co-Advisor

Keywords:

1. Formula Hybrid
2. Frame Design
3. Accumulator Design

# Acknowledgements

We would like to thank our project advisors, Professors William R. Michalson, David C. Planchard, and Andre Rosendo for their guidance, insight, and for keeping us on track throughout the academic year. We would also like to extend our thanks to Ian Anderson for his indispensable guidance and expertise in manufacturing, Colleen Shaver for her unwavering support, and Barbara Furhman for facilitating all our various purchasing requests. A final thank you is due to the members, both current and past, of the WPI Society of Automotive Engineers for their support.

# Abstract

The Formula Electric MQP designed and manufactured a new electric race car from the ground up. The car will compete in Formula Hybrid+Electric, an interdisciplinary design and engineering challenge which allows students to put theory to practice, utilizing kinematic analysis, 3D design, and CNC manufacturing. The team's goal was to create the highest performance electric race car WPI has ever seen, putting an emphasis on reliability and serviceability so the car can be used as a foundation for a future MQP. This year's car was designed, manufactured, and tested from the ground up. We created a new frame, a custom battery pack, systems for suspension, braking, and steering, as well as full bodywork. We optimized vehicle systems using data collected from previous cars to reduce vehicle weight while improving performance. We achieved our goals of reducing weight by 10%, increasing lateral and longitudinal g-forces by 20%, and remaining reliable and serviceable.

# Executive Summary

This year's Formula SAE Racecar project represents the third effort by members of the Worcester Polytechnic Institute to bring an all-electric formula-style vehicle to competition. While WPI has a long and proud history of competing in SAE design competitions – both Formula and Baha – we are comparatively new to the all-electrical space (WPI Formula SAE).

The process of creating this year's vehicle began with the design and outsourced assembly of an entirely bespoke frame. This frame was designed to accept our pre-selected components, a process that required significant planning foresight. The geometry of the frame was designed based on a combination of prior experience, established procedures, and compliance with competition regulations. In addition to designing the bare tube frame, we designed, manufactured, and welded all our frame tabs.

With the frame design solidified, the mechanical team's attention turned in earnest toward the parallel design of our new driver cell, wheel packages, drivetrain, steering, and bodywork. Working on these systems in parallel required extensive intrateam communication, knowledge sharing, and design reviews.

In addition to working cohesively within the mechanical team, integration of electronic systems necessitated a continuous flow of information between teams. The tasks completed by the electrical team this year include the design and production of a bespoke accumulator, Accumulator Management System, sensor boards, digital user interface, rules compliant TSAL, and a robust shutdown control system. Each of these tasks presented unique challenges that were overcome by way of extensive collaboration, analysis, and information sharing. Ultimately, we produced a cohesive, adjustable, and highly performant vehicle.

# Table of Contents

# Table of Figures

# Table of Tables

# Background

The Formula Hybrid + Electric Competition is an SAE design and engineering challenge. Students from across and beyond the US design and build formula-style race cars to compete in a series of events hosted annually at the end of April in Loudon New Hampshire. The WPI FSAE team has been around since 1976 competing with many internal combustion vehicles (WPI Formula SAE). Beginning in 2020, we moved away from internal-combustion-based competition, joining the aforementioned competition. This transition to a heavily interdisciplinary competition has taught us a great deal about how to manage a team composed of students from four different majors. Additionally, this new type of competition brought an entirely new set of regulations and safety concerns that we have worked diligently to abide by.

Based on prior experience, the team identified the need to create a more accessible and adjustable vehicle (WPI Formula SAE). More specifically, in our competition environment, we take part in an endurance driving event that requires multiple drivers to take the wheel. To that end, our vehicle needs to not just be adjustable but rapidly adjustable. Additionally, we want our vehicle to be easy to work on. With those needs in mind, we created a new highly optimized frame & suspension, improved accumulator, robust powertrain assembly, carbon fiber body, bespoke pedal box, and many more systems that are discussed at length in the body of this report.

# Process

## Frame

The frame for EV24 was designed based on the 2019 Internal Combustion car known as “Margarita” (WPI Formula SAE). Most of the initial design took place over two terms of ISP’s in 2023 C and D-term. The ISP team set out to design a frame that could house a large accumulator while attaining a minimum allowable wheelbase (1524mm) and accommodating high performance suspension.

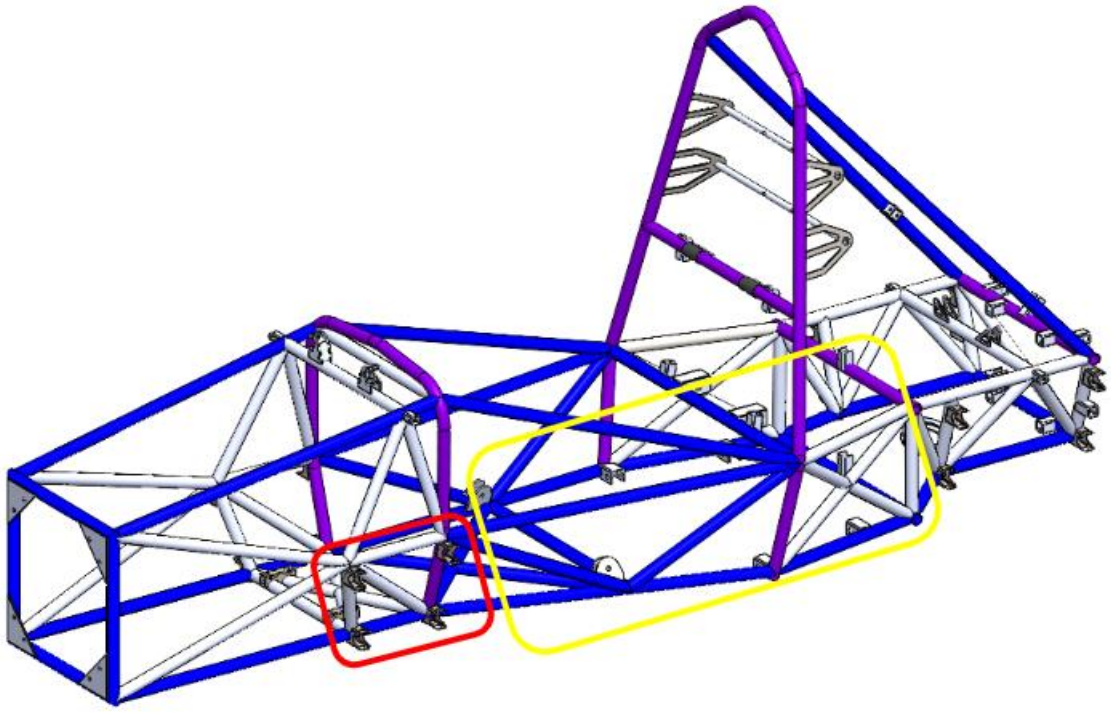

*Figure 1: Frame Design*

The design for the frame began at the wheels and the accumulator and worked inwards. The accumulator housing dictated the envelope of space we would need to leave open, in addition to installation space. The wheels dictated the uprights, suspension type, and frame pickup points. The team then attempted to include as many components as possible to ensure we could appropriately package them.

The final iteration of the frame has a couple major changes from previous years.

The changes are boxed below. The red box shows the tight packaging of the front control arm pickup points. This was to accommodate one of our suspension design goals of minimizing scrub radius. To do this we needed to reduce the backspacing of the upright within the wheel, effectively pushing the upright further towards the center of the wheel. This meant that we would need far more acute A arms to allow for a sufficient steering angle. Since we want to minimize compliance and bending within our tube chassis, the suspension pickup points are best placed on or very near nodes. This led to the front box looking the way it does. Boxed in yellow is the large area for the accumulator. The big change here is that all of our previous frames have had a member at the bottom of the roll hoop. This year we decided to make that member a removable member that is attached to the accumulator. This allows for high strength of the hoop and mid chassis when the accumulator is installed while also allowing for easy mounting of the accumulator. This also allowed us to package the accumulator much farther forward in the chassis. This is the reason we were able to achieve a wheelbase of 1530mm, just 6mm over the minimum for safety in compliance.

When designing the frame we paid very close attention to proper triangulation as it had been a sticking point of the team on every chassis since 2020. This paid off as our SES submission was approved on our first try, giving us 20 bonus points for early submission.

For further information of the development behind the frame refer to the C-Term EV24 ISP Report.

## Frame Tabs

Much of B-term was spent manufacturing and welding on frame tabs that are critical to the rolling chassis by the end of the calendar year goal. As of now all control arm tabs are tack welded in

place, as well as the rear toe tabs and front shock tabs. These are pictured below. By the end of the calendar year, the front rack tabs, rocker tabs, and rear shock tabs will all be tacked in place and then fully welded.

## Impact Attenuator

The purpose of the impact attenuator is to safely decelerate the car in the event of a head on collision of up to a 40G impact. Four triangular shaped plates are welded in the corners of the front bulkhead to mount the anti-intrusion plate to. These plates are 1/8” 4130 steel. Our anti-intrusion plate is a 6061-T6 aluminum plate with a thickness of 0.157”. The impact attenuator is an aluminum honeycomb structure purchased from Plascore. The honeycomb structure is glued to the anti intrusion plate using E6000 construction adhesive.

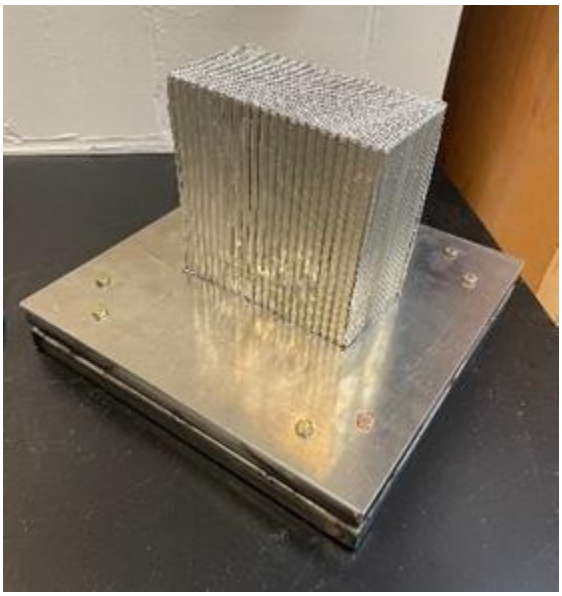

*Figure 2: Impact Attenuator Test Fixture*

With help of the civil engineering department, we used an Instron to crush the test impact attenuator. The impact attenuator successfully absorbed the force and the anti intrusion plate permanently deflected less than 1 inch.

*Figure 3: Impact Attenuator Test Setup*

*Figure 4: Impact Attenuator Test Result*

After the crush test, we were required to generate graphs from the data to show Load vs Displacement and Energy Absorption. These graphs show what was expected since there is no peak deceleration with this impact attenuator.

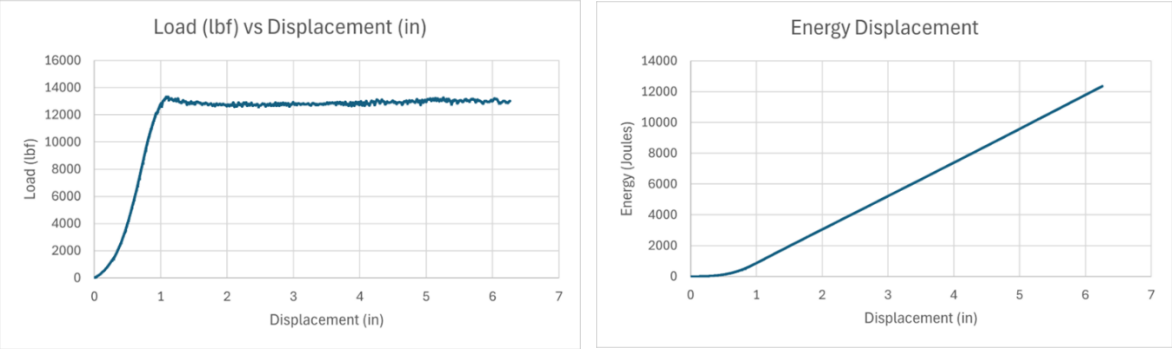


*Figure 5: Impact Attenuator Test Data*

Required calculations, courtesy of the competition rules, are shown below:

**Given Rules Information:**

- Velocity: 7 m/s
- Average Deceleration: < 20G
- Peak Deceleration: <40G

**Given Manufacturer Specifications:**

- Crush force: 375 psi ($2.59 * 10^6 \frac{N}{m^2}$)
- Max crush stroke: 70%

**Assumed weight:** 700lbs (317.51kg)

Total Vehicle Energy

$$KE = \frac{1}{2}mv^2 = \frac{1}{2}(317.51kg)\left(\frac{7m}{s}\right)^2 = \mathbf{7779\ Joules}$$

Total Energy Absorbed

$$Max\ Stroke: (0.7)(0.203m) = \mathbf{0.1421m}$$

$$Work = (Force) * Displacement$$

$$Work = (Crush\ force * Area_{cross\ section}) * Max\ Stroke$$

$$Area_{cross\ section} = \frac{7779\ Nm}{(0.1421m) * (2.59 * 10^6 \frac{N}{m^2})} = \mathbf{0.0211m^2}$$

$$Width\ Requirement: 0.0211m^2 = (0.2m * \mathbf{0.1m}) + (0.2m * \mathbf{0.0057m})$$

$$Total\ Width\ of\ IA\ to\ absorb\ impact: \mathbf{105.7mm}$$

*Figure 6: Impact Attenuator Energy Absorption Calculations*

Average Deceleration

$$V_x^2 = V_0^2 + 2a(x - x_0)$$

$$0 = (7\frac{m}{s})^2 + 2(G * 9.81\frac{m}{s^2})(0.1421m)$$

$$\boldsymbol{Average\ Deceleration: 17.59G}$$

Note: We can assume that there will be no peak deceleration throughout this impact because this Plascore impact attenuator is advertised to not have an initial peak impact. This is confirmed through our testing in our Energy vs Displacement graph.

*Figure 7: Energy Absorption Calculations Continued*

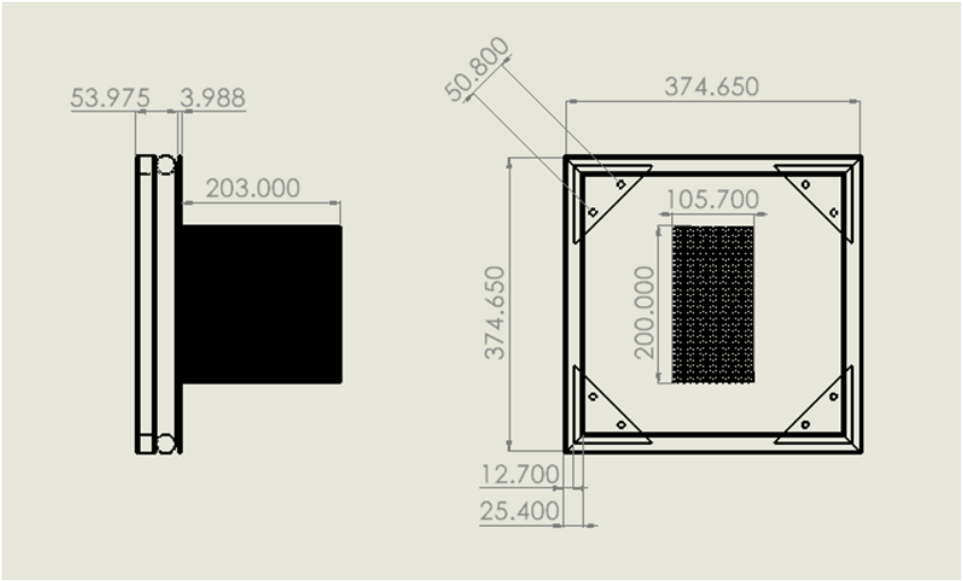


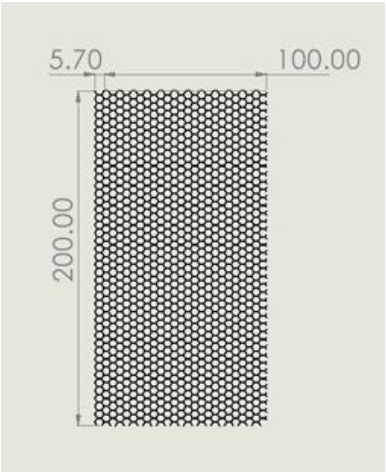


*Figure 8: Impact Attenuator Test Assembly CAD Drawings*

## Accumulator Mounting Strategy

The design of an easy-to-maintain and robust accumulator is a critical part of competition rules compliance. The main goals for this design was to reduce the number of bolts required for installation by designing a removable frame member. Through group discussion, a basic strategic overview was developed. Specifically, our attachment strategy consists of two bolt-in crossmembers on the bottom of the accumulator and two substantial brackets on the top of the accumulator.

Seen immediately below left is the critical path of fasteners between the frame and the bottom of the accumulator enclosure and below right is the critical path between the frame and the top of the accumulator enclosure.

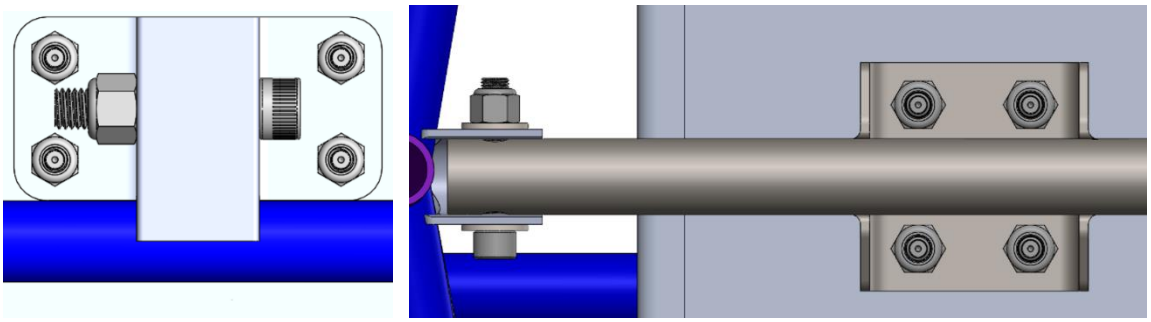

*Figure 9: Accumulator Hardware Critical Path*

A modification to the team's initial design was required due to a missed clearance issue. Specifically, in the following figure, the frame tabs that retain the smaller bolt-in cross member interfered with the accumulator enclosure. In order to minimize alterations to the accumulator enclosure and our overall strategy, the following design was created:

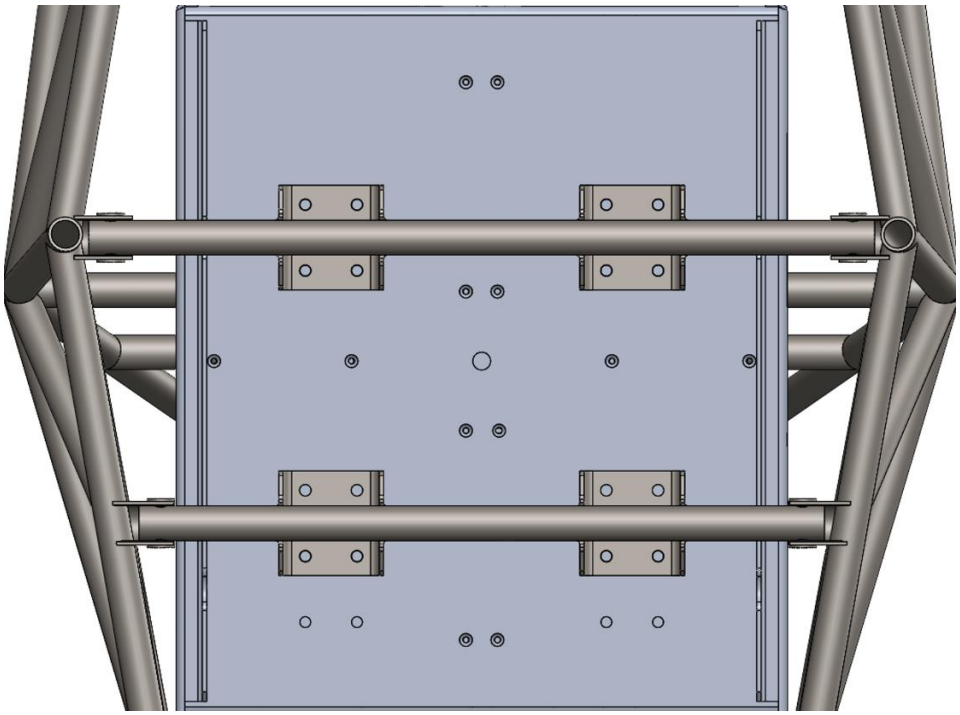

*Figure 10: Improved Accumulator Mount*

While tolerances were forced to become quite tight, the above design proved to be equally if not more robust than the prior iteration. Additionally, it necessitates the drilling of only four new holes as opposed to the full eight and a small radius cut to clear the new relative position of the steel tube. In order to confirm compliance with pre-competition SES documentation, a full suite of load studies was conducted:

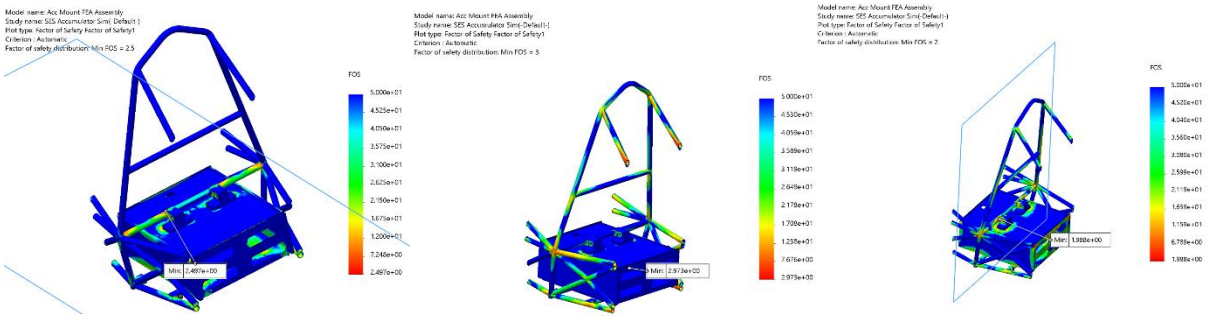

*Figure 11: Accumulator Mount FEA Results*

The team has now successfully installed and uninstalled the accumulator on multiple occasions indicating that the modifications were successful.

## Jack Bar

Being able to quickly and efficiently jack the car up for maintenance considerations will allow the team to operate seamlessly. The jack bar mounting tabs were the first thing designed, they consist of four welded tabs designed in SolidWorks Weldments, they will be CNC machined out of 4130 steel plate allowing a seamless interface between the frame and the tabs. These tabs will hold a set of two CNC machined aluminum pieces. Finally, these aluminum pieces will be welded to the horizontal jack bar and brace plate. Assuming a 226 kg car, static analysis was conducted to determine that 883 N force is required to lift the car. Finally, FEA was conducted on the jack bar assembly to validate its resistance to these loads.

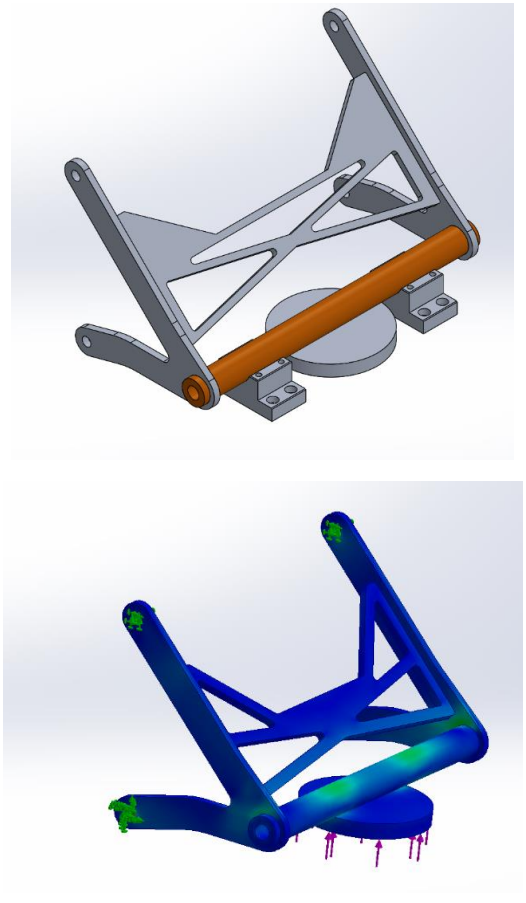

*Figure 12: Jack Bar Assembly and FEA Simulation With Floor Jack Puck*

# Driver Cell

Based on prior experience, the team identified the need to create a more accessible and adjustable vehicle. More specifically, in our competition environment, we take part in an endurance driving event that requires multiple drivers to take the wheel. To that end, our vehicle needs to not just be adjustable but rapidly adjustable. There are also extensive rules compliance concerns that must be considered when effectively designing each aspect of the vehicle that the driver interacts with.

## Headrest

Ensuring comfort for drivers of all sizes on the team and rules compliance were the two main goals desired in the EV24 headrest design, we also valued a lightweight design, as the head rest resides high in the vehicle, amplifying effects on CG. The headrest design consists of 4 waterjet 4130 tabs that are welded to the roll hoop, these tabs are welded to 2-4130 cross member tubes consisting of 2 holes in each rod for ⅜” through bolts. These rods are encased by 2 aluminum CNC machined parts that span the width of the head rest. To achieve adjustment for various size drivers, an assortment of 4130 tubes will be used in which the ⅜” bolt will be placed in. To spread the load from the head rest plate and the tubes, another aluminum CNC machined part (the same as part as on the other side of the tube but with no cutout for the cross member) will be used. Headrest components were run through an FEA simulation based on competition rules.

*Figure 13: Assembled Firewall/Headrest*

## Firewall

The team extensively reviewed the rules for firewall design before strategizing a design. The design was first modeled using SolidWorks Sheet Metal features, this extremely valuable software allows the bent, finalized part to be “unfolded” in order to manufacture it out of a sheet of material. The rules state that the firewall must be 1.5mm (0.059”) aluminum or thicker, to avoid having to prove another material for fire resistance, the firewall will follow these material parameters.

The firewall will be mounted using a few different fasteners, starting from the bottom, integration with the floor via a separate flange of bent aluminum will allow both the firewall and floor to be separately mounted, but also allowing one to be able to be removed without the other. The middle section of the firewall will be secured with a loop clamp around each side of the frame and a through bolt through the firewall. Finally, the upper section of the firewall will integrate with the headrest bolts by sandwiching between one of the plates and a spacer or tube, depending on what configuration the firewall is in.

To validate the design, a laser cut cardboard mock firewall was made to ensure fitment and rules compliance. Using a router, we were able to manufacture an aluminum firewall and then bend it into form. Being able to visually see an almost completed design on the car was valuable in creating seamless integration, rules compliance and fit.


*Figure 14: Firewall Installed with Seatbelts & Headrest*

The lowermost portion of the firewall also includes a cutout section to accommodate the addition of our passive accumulator cooling strategy, seen below. The added flange is made out of the same aluminum used for the body of the firewall and attached by rivets and aluminum tape to achieve full rules compliance.

*Figure 15: Accumulator Duct Cutout*

## Structural Floor

The team deemed it necessary to design and implement a structural floor constructed of aluminum in order to avoid damaging our carbon fiber bodywork. Initially a cardboard template was cut and used to determine how far the frame model strayed from it's as-welded configuration. Images of this template and it's testing can be seen below.

*Figure 16: Structural Floor Template*

This test fitting exercise allowed the team to determine the locations of necessary relief cuts, shown in the following pair of images.

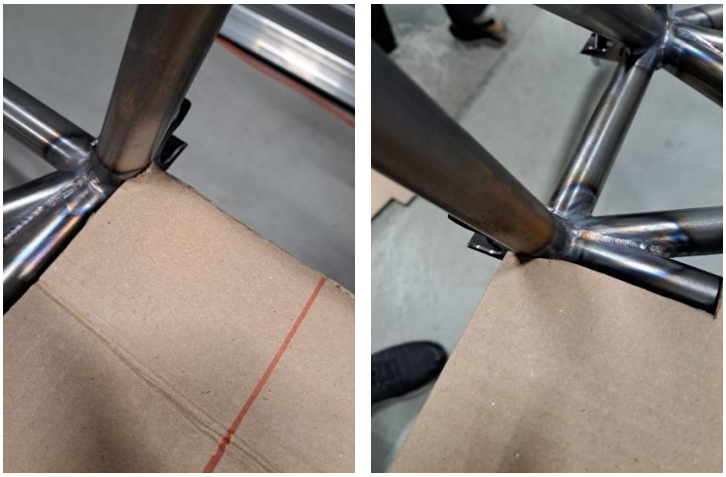

*Figure 17: Structural Floor Test Fit Results*

Using the data from that test, the team decided to move forward with laser cutting an initial revision using an aluminum plate. The following drawings were created after hardware alignment was checked in CAD and alterations were made to ensure user safety:

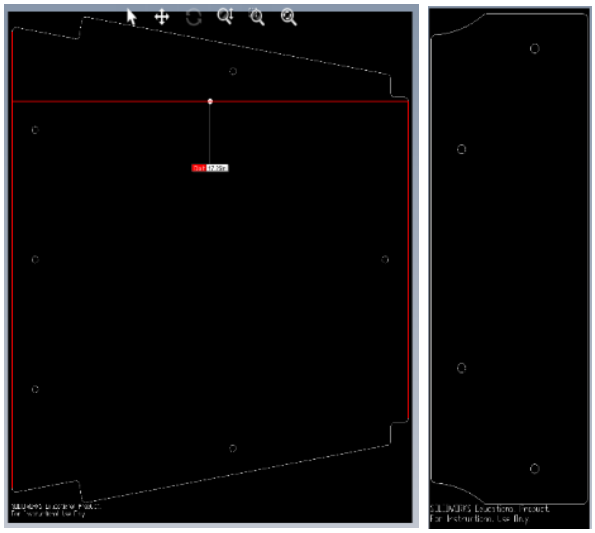

*Figure 18: Structural Floor CAD*

Upon the arrival of the required mounting hardware the panels were fitted into the vehicle.


*Figure 19: Aluminum Floor Assembled*

The rearmost portion of the aluminum floor was also bolted to the firewall flange. The flange itself was a simple hand-bent piece of aluminum with holes that were drilled in situ. The intention of the flange is to allow for independent installation and removal of the firewall and structural floor.

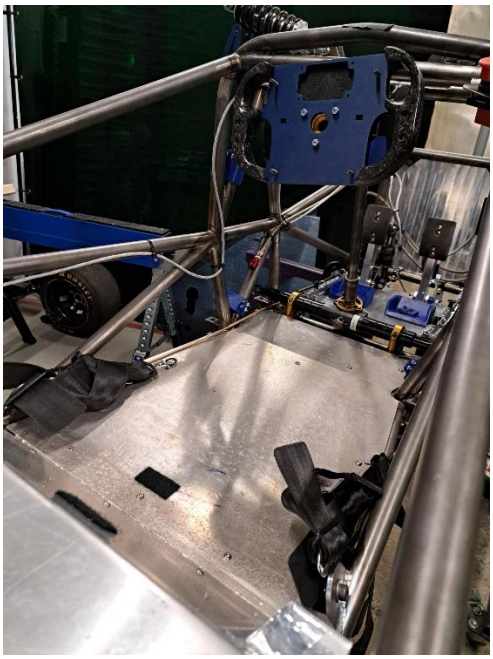

*Figure 20: Final Aluminium Floor Assembly*

## Pedal Box

Another major focus of the team's efforts this term was finalizing the design of our pedal box. In order to finalize the design, the team's first step was to confirm a) the ideal range of motion from the shortest to the tallest driver and b) identify the location of our ideal pedal locations relative to fixed points on the frame. Upon conducting fitment tests with multiple drivers, data was gathered and it was determined that an under-floor master cylinder arrangement was unfeasible. As such, an extensive review of prior art was conducted to determine the most compact manner in which FSAE brake systems can be packaged. Ultimately, an inverted master cylinder/balance bar arrangement was decided upon inspired by the work of fellow Formula SAE competitors from the University of Akron (Demetriades et. al, 2020).

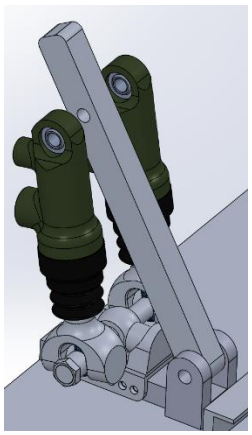

*Figure 21: Inverted Pedal Arrangement Test Assembly*

SolidWorks sketches were used to iterate through designs in order to optimize our pedal leverage ratio in such an unconventional setup. Ultimately, a leverage ratio of 3.56 was determined to be optimal from a mechanical perspective, a figure that is well within the range of those typically used in FSAE vehicles.

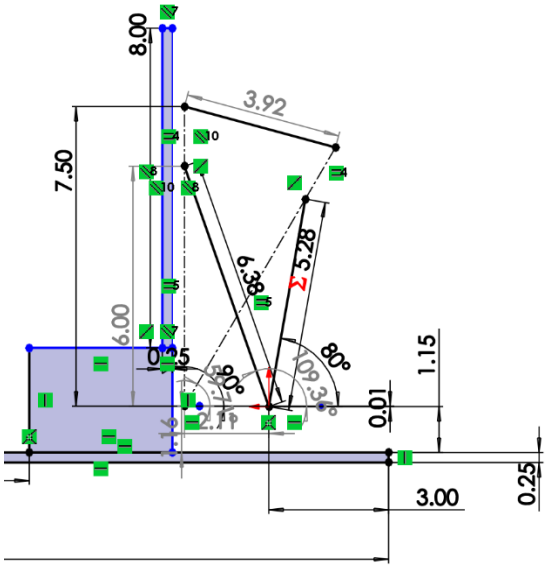


*Figure 22: SolidWorks Leverage Ratio Calculation*

Ultimately, through the efforts of several team members, the following design was created. This design satisfies all relevant rules and will easily accommodate all our drivers. It includes bespoke

pedals as well as an OEM-style throttle pedal arrangement. When coupled with our adjustable headrest, steering box bracket, and seating arrangement, we achieved a high level of accessibility.

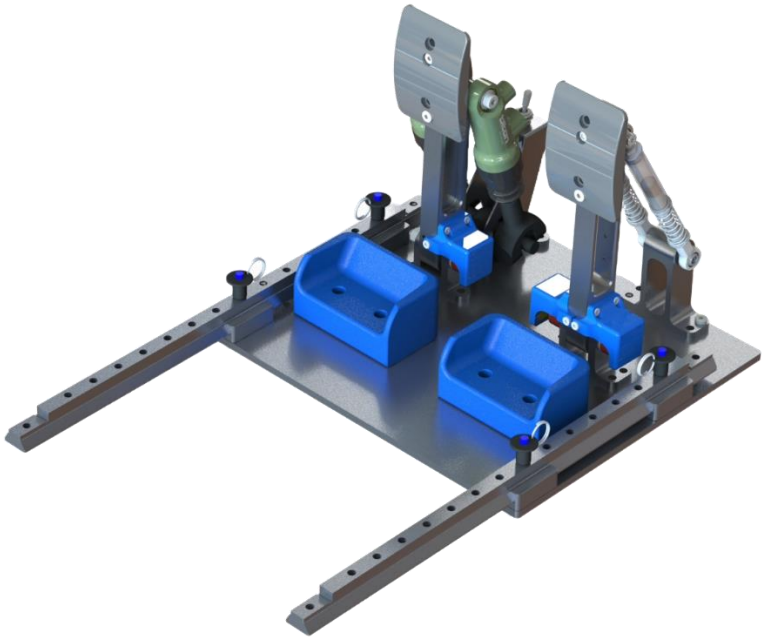

*Figure 23: Final Pedal Box Assembly*

## Seat

In keeping with our goal to create an accessible vehicle, a total of three seating solutions were prototyped and manufactured to accommodate our wide range of diver sizes. The simplest of these solutions, dubbed the “potato wedges,” can be seen below.

*Figure 24: Potato Wedges*

This seating strategy is designed to accommodate our tallest and widest drivers while remaining rules compliant. For our smaller drivers, two seats were created based on fiberglass sprint-kart racing seats. These seats were heavily modified using structural foam reinforced by layered carbon fiber.

*Figure 25: Alternate Seat*

The design of the seats was based around complying with the competition rules for head position and all relevant belt angles, testing of which can be seen in the following collection of images.

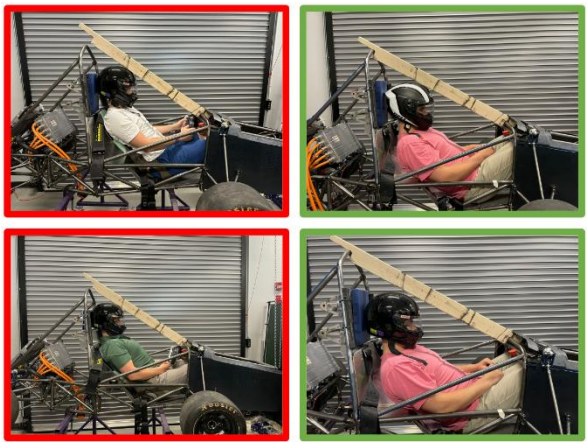

*Figure 26: Seating Position Testing*

# Wheel Package

We began the concept of our car with the tires, moving inwards as the design progressed. From the start, we had three primary goals that affected our wheel package design. First, we wanted to sustain 1.7 G lateral and 1.5 G longitudinal loads. We chose these numbers because they represent a marked performance increase over our previous electric car and are similar to measured loads on our team's past successful ICE cars. Second, we wanted to minimize steering effort, allowing our drivers to maintain precise inputs throughout the endurance event. Finally, we wanted to allow for as much adjustability as possible to tweak parameters after on-track testing.

## Suspension

For the suspension of EV24 the team eventually settled on pushrod actuation front and rear. We looked at an extensive number of options during the ISP but the benefits of Pushrods ease of packaging and constantly planar forces outweighed the cons of slightly raising the CG and having tubes in compression. The team also decided to go with two-part rockers, allowing for the use of waterjet cutting to reduce the long list of parts to CNC machine. The front suspension is pictured below. There are a few notable design elements. First the shocks are laid down so the reservoir does not impede the driver's line of sight. This led to the design of the front shock tower tabs (pictured in a red box). The tab will be waterjet-cut out of 4130 ⅛" plate and will slot together to be welded. The tab incorporated two lower plates, one of which will house a captive ny-lock nut. This reduces the need for a spanner when assembling the suspension. Another design element is the use of thrust bearings (circled in blue) at the rocker pivot. Since the rocker will be made in two parts, they will need the bearings to allow for rotation once the pivot bolt is tightened. This should also further mitigate any sideloads from imperfect manufacturing or welding. The final notable element is the use of "top-hat" spacers on either end of the push rod (pictured in pink, within the

blue box) These spacers replace a purely cylindrical spacer and washer, while enabling the team to ease assembly and to work around shoulder bolt tolerances for a tighter fit.

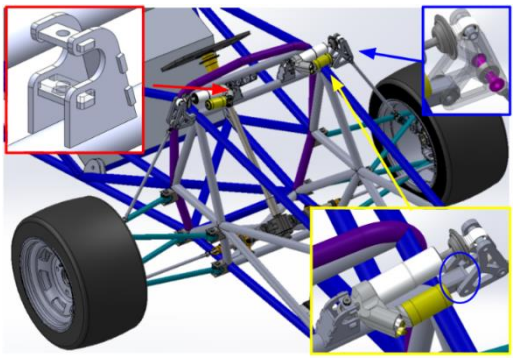

*Figure 27: Suspension Design Overview*

## Control Arm Manufacturing

During B-term we manufactured all the needed bearing cups with an increased efficiency manufacturing method. This year the ST30 with bar feeder was used to make bearing cup slugs that had been pre-drilled, OD turned, faced and parted to length. The bar feeder allowed us to pump these out largely unattended once the process was refined. The slugs were then machined in a set of custom soft jaws for OP 1 and OP 2. The slugs and finished parts can be seen here.

*Figure 28: Bearing Assembly & Manufacturing Process*

To validate the critical dimensions relating to the bearing staking process, two gauge-blocks were turned to tight tolerances. These blocks could then be used with a micrometer.


*Figure 29: Manufacturing Validation*

All the tubes were cut on the VM-2 using custom soft jaws, this allowed each tube to be cut in one operation. Numerous cross members and control arm tabs were also machined.

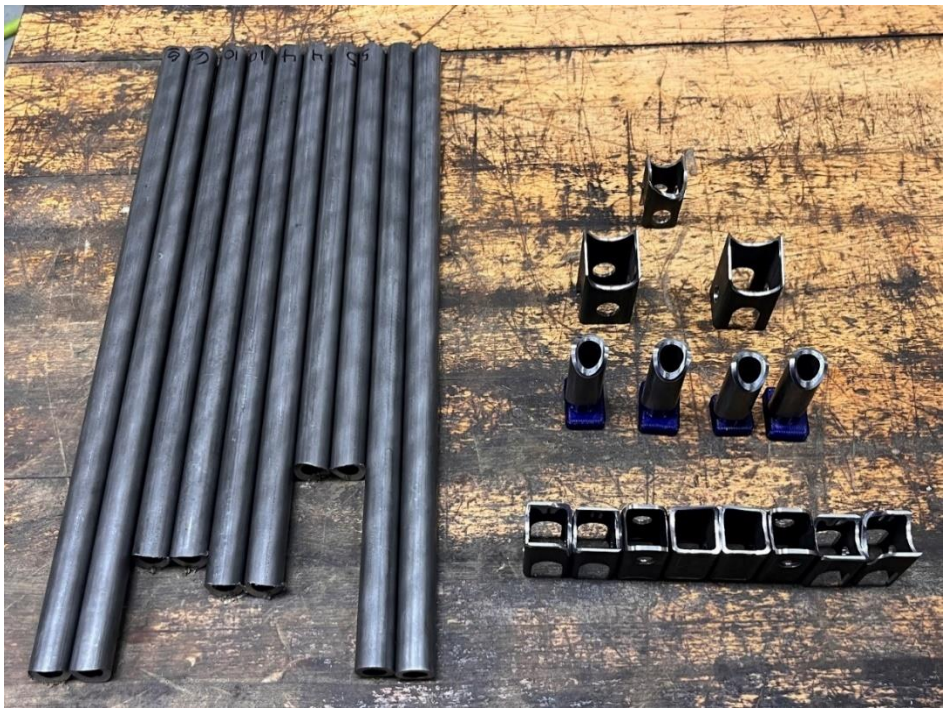

*Figure 30: Control Arm Component Manufacturing*

A welding fixture was also machined and assembled to aid in the accuracy of welding. Bushings to fixture the bearing cups were turned and tube clamps were machined. Laser cut cardboard templates were also cut to help with the alignment of the bearing cups.

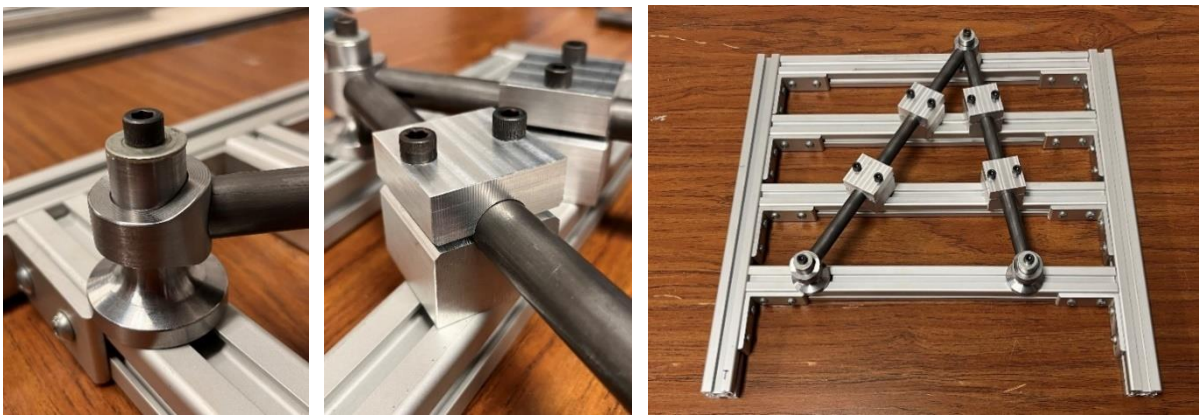

*Figure 31: Control Arm Welding Fixture*

*Figure 32: Control Arm Welding Results*

## Uprights

The uprights are an integral part of the car. They are the link between the control arms and wheel hubs. Any force on the wheel is directly transferred into the car through the path of control arms, suspension, and tie rods. The uprights have a much different design between the front and rear uprights. The front uprights (left) accommodate a tuned scrub radius, kingpin inclination, camber, and castor. To accommodate for specific locations of mounting points, the uprights were formed around these specific qualifications. The rear uprights (right) are much simpler since the rear wheels do not steer.

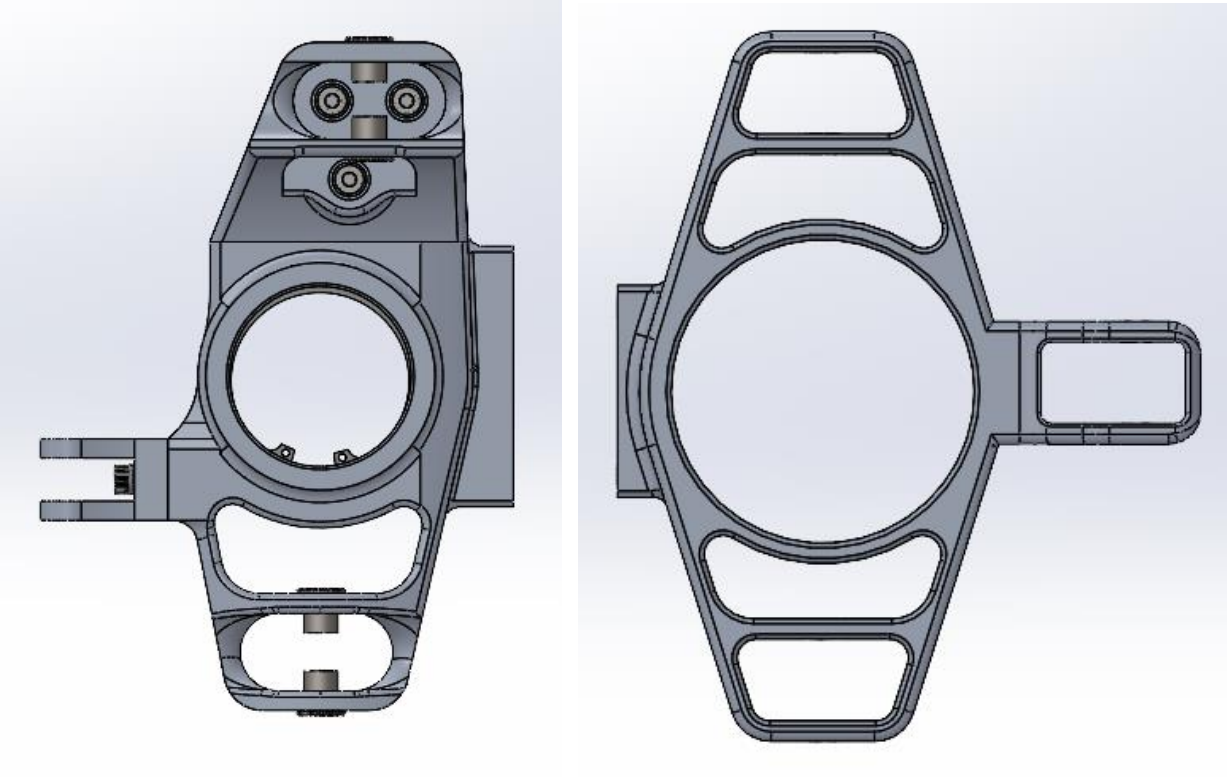

*Figure 33: Front Uprights in CAD*

The front uprights use a modular design where the upper mount for the control arm and the tie rod mounts are bolted to the main body of the upright. This gives us more flexibility in the future to iterate our upright design without remanufacturing the entire upright. A second benefit of the modular upright is that we are using much less stock to make these parts. We would have had to use at least a 3” thick block of aluminum. Now we are able to use 1.25” thick stock that the team already owns.

The upper control arm mount is fastened to the body of the upright using 3, 5/16-18 low profile socket head bolts. These are through bolted to ensure maximum strength as opposed to threaded aluminum. The mount also utilizes a mortise and tenon style groove (bordered in red) to align the mount and help manage longitudinal and vertical forces.

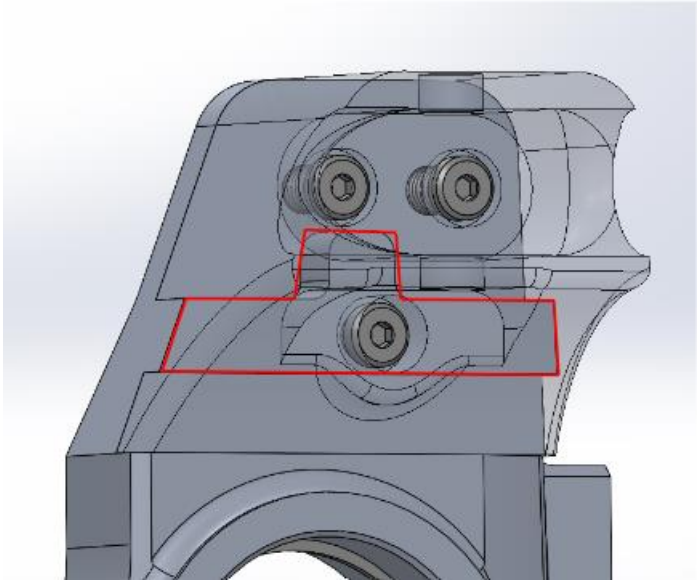

*Figure 34: Mortise and Tenon-Style Groove*

The modular tie rod mounts also have this same mortise and tenon joint to offload some of the forces off of the bolts (bordered in blue). The joint is especially useful in this mount because the bolts are threaded right into the upright body. The bolts will be getting a full inch of thread purchase which is much more than twice the bolt diameter as recommended.

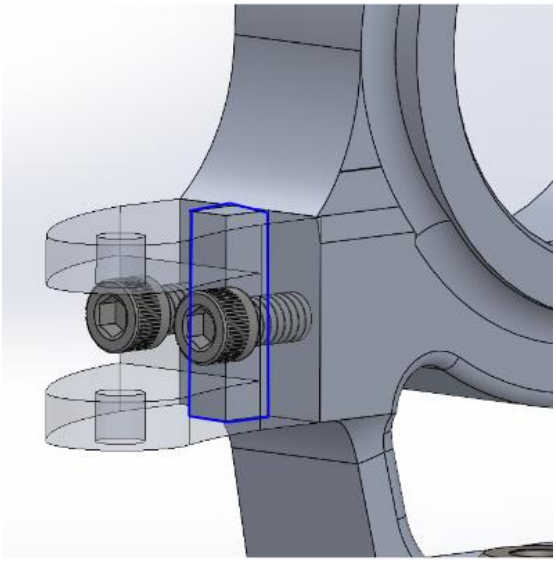

*Figure 35: Tie Rod Mount CAD*

The FEA results on the front uprights were very important to get correct. This is our first time using modular uprights on our car. Using the joints and through bolts when we can ensure a strong connection between the mounts and the upright body. As seen below, while running a static analysis of the upright, the connection points at the control arms and tie rod are fixed. All forces are applied to a dummy hub to accurately transfer the forces as they would be in real life on the car. Bolted connections are used where bolts will be present and local interactions are used to better define this scenario. Forces on the dummy hub are as follows:

- Lateral: 6,340N (2g force, assuming 700lb/317kg car)
- Longitudinal: 6,340N (2g force, assuming 700lb/317kg car)
- Vertical: 9,510N (3g force, assuming 700lb/317kg car)

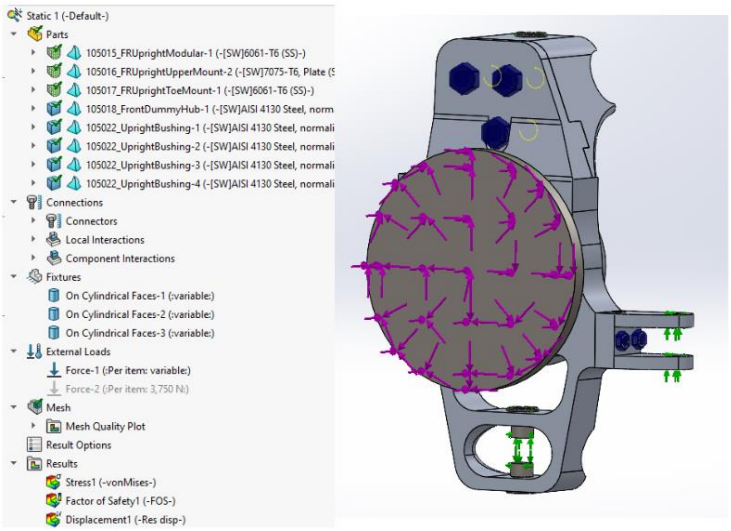


*Figure 36: Upright FEA Setup*

Using this setup, we get a minimum factor of safety of 2.7. Since this is a major part of the car a higher factor of safety is acceptable, compared to our target FOS of 1.5 on smaller and less critical parts. Using the same setup as the front uprights on the rear, we get a minimum factor of safety of 3.5.

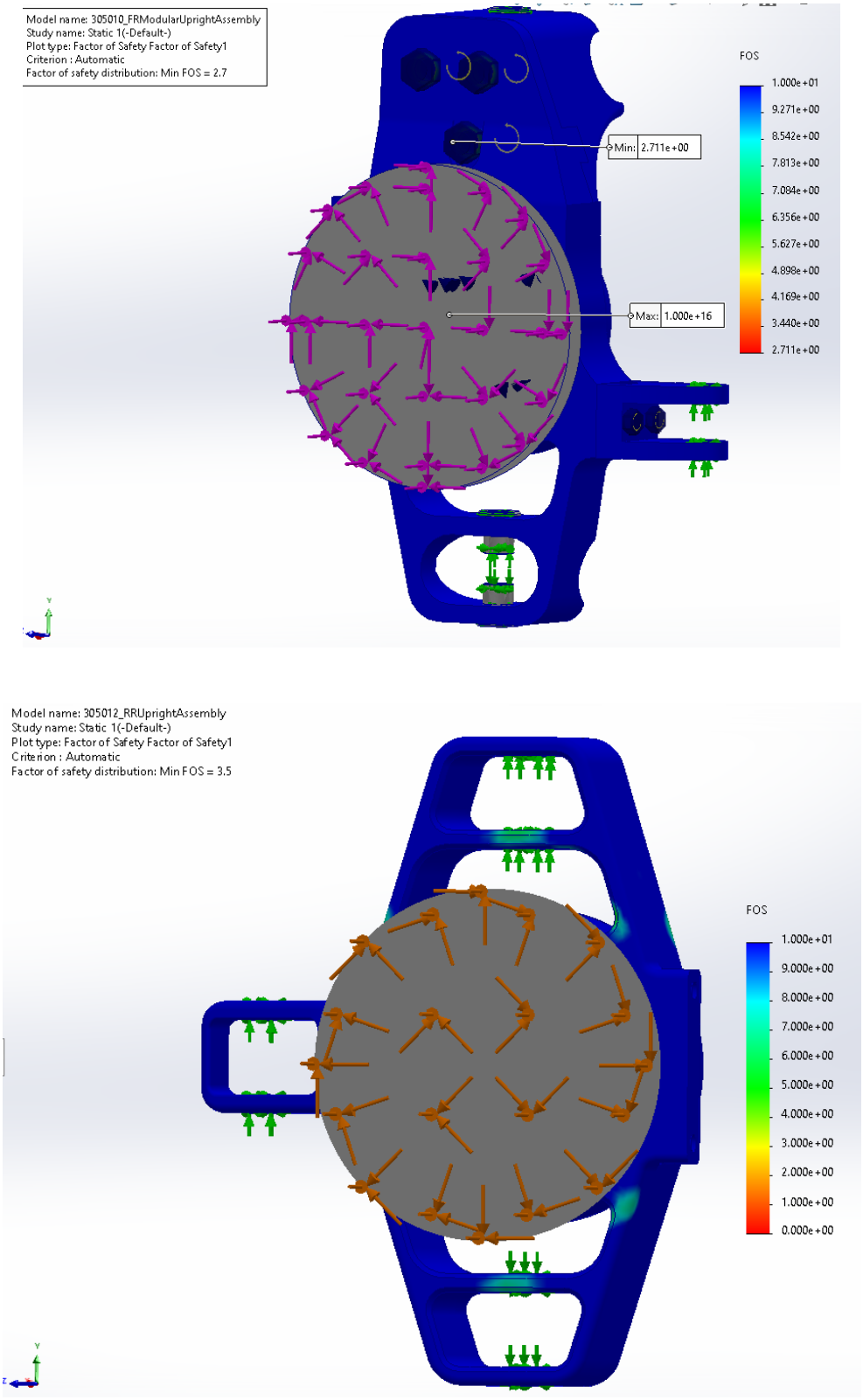


*Figure 37: Upright FEA Results*

## Drivetrain

Designing a robust and continuously adjustable powertrain design was one of the first tasks that the team undertook. As such, mounting strategies for the differential and the motor were delegated to separate members of the team who learned to work closely on their tightly integrated tasks. Through an iterative design process informed by prior art studies and extensive FEA bespoke mounting strategies for both major drivetrain components were produced. These systems were manufactured fully in-house and have already proven functional. It is important to note that in validating these components the team focused on designing mounts that would survive the impulse loads that they experience on track.

### Differential and Mounting

The differential is of critical importance as it allows the wheels at each end of our rear drive axle to rotate at different speeds, which is crucial for the car to maintain torque during cornering.

The choice of differential was straightforward as the team decided to carry over the previous year's component. This was our decision because our differential, the *Drexler Adjustable FSAE Differential V2/V3*, is already regarded as one of the best due to its adjustability, and because it is a cost the team does not need to incur.

This component is intended to be held by our differential mounts that fixes its position relative to the frame. This must be done in a robust manner as any form of movement by the differential might cause reliability issues with the rest of the powertrain system. Additionally, this mount will not only secure the differential in place but will also hold the driveshaft of the vehicle.

Another use case for the differential mount is to allow for chain tensioning. Although chain tension can also be achieved with an idler or a spring-loaded sprocket that pushes down the chain, there

are benefits of doing it with the diff mount. An idler introduces more moving components to the powertrain alongside additional weight whereas a smart differential mount design can achieve the same while not introducing new failure modes to the powertrain. Because of this, we have chosen to leverage the differential mount to create chain tension.

This is achieved by moving the driven sprocket away from the driving sprocket. The team has done two different approaches in the past, each with its pros and cons as shown in the table below:

*Table 1: Differential Mounting Strategies*

| | **Eccentric Tensioner** | **Continuously Adjustable Tensioner** |
|---|---|---|
| **Pros** | Easier to maintain both mounts parallel | Has continuous adjustability allowing us to consistently obtain ideal chain tension. |
| **Cons** | Discrete chain adjustment | Depending on the approach, it will be hard to maintain mounts parallel |

After multiple discussions we decided that the main objective for this year was to be better at limiting the DOF of the mounts. The continuously adjustable tensioner is the ideal choice, but it was crucial to design it so that there was no room for error when adjusting the chain. Additionally, choosing to go with a continuously adjustable tensioner approach does not prevent us from using an eccentric tensioner as both can be combined.

## Differential Mounts Design

A lot of time and focus was dedicated into finalizing and freezing the differential mount design. Original struggles stemmed from: overlooking the need to conduct FEA analysis of the mounts on an assembly level within the frame, not accounting for impulse loads, choosing and sourcing turnbuckle components, and frame tab design.

The design began by determining the reaction forces at the mount. These resulted from the chain tension during acceleration and the weight of the components supported by the mounts. The chain tension was calculated as follows:

$$\text{Chain Tension} = \text{Motor Torque} \times \text{Radius of Driven Gear}$$

After obtaining the chain tension, we then used the equations of equilibrium to determine what would be the reaction forces at the mounts. To do so we first had to establish a coordinate system:

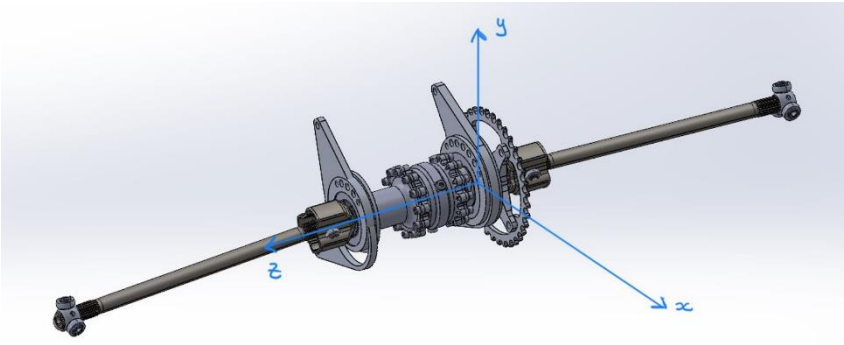


*Figure 38: Coordinate System for Differential Assembly*

Once that was done, we determined the center of gravity of all components in the differential assembly, their weights, and their relative positions to the left differential mount.

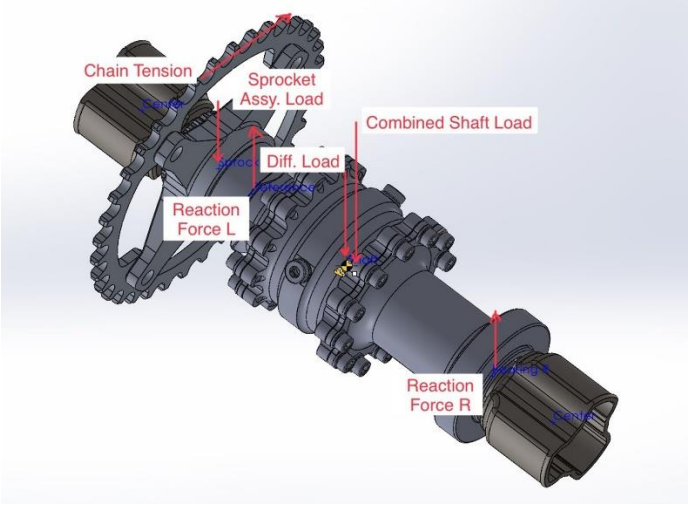


*Figure 39: 3D Freebody Diagram of Differential Assembly*

Lastly, the reaction forces were solved by writing a MATLAB script based on force and moment equations. The resulting forces were then used to create initial designs for both the turnbuckle and differential mounts.

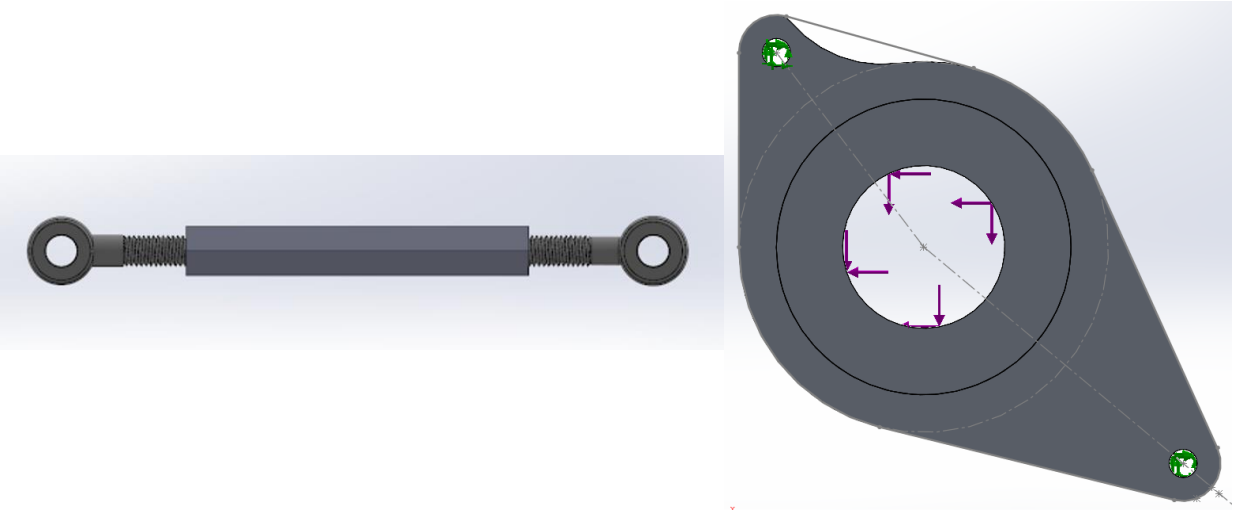

*Figure 40: Final Designs by the End of A-Term 23/24*

Early into B-Term, the team observed severe deformation and other structural issues being caused to the frame by the motor mount, and at this point impulse loads were not being considered either. As the differential and motor mounts exhibit the same behavior and experience the same force in opposite directions we conducted a differential mount and frame assembly analysis.

The setup of the analysis required several “dummy” components such as the dummy differential assembly to be created. Moreover, to take into account impulse loads the team followed the approach recommended by several forums and our professors to model it as double the expected load. Without the impulse loads taken into consideration I obtained the following results.

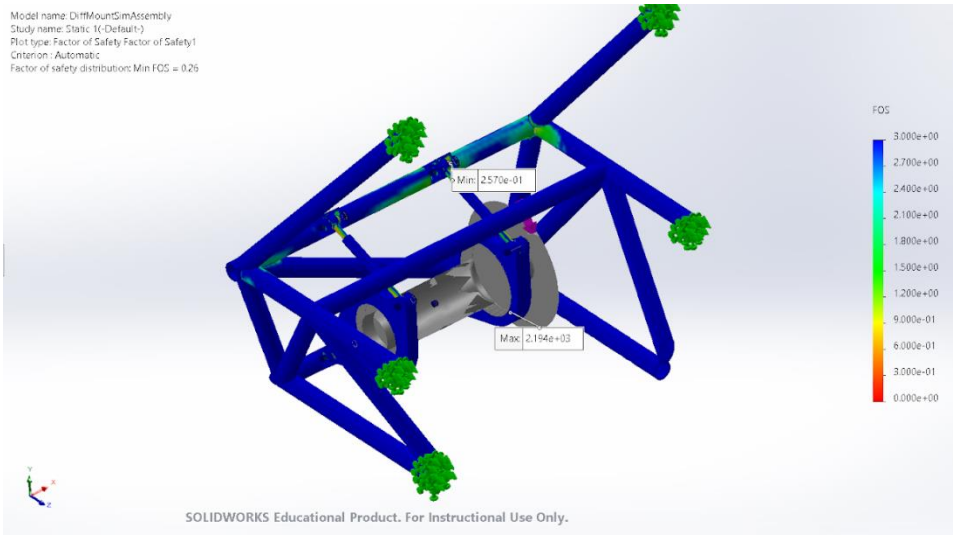


*Figure 41: FEA Analysis of A-Term Mount in Frame*

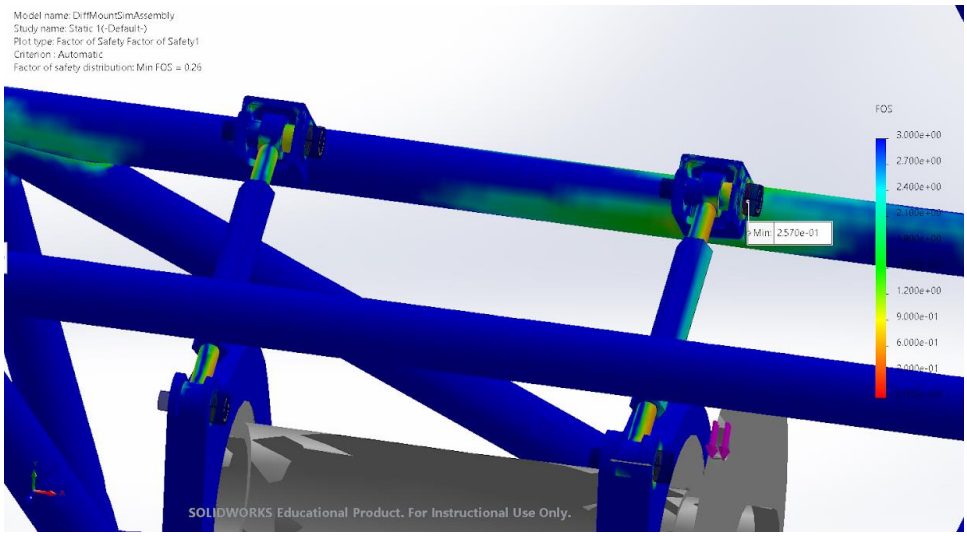


*Figure 42: FOS of Turnbuckles FEA Analysis of A-Term Mount in Frame*

As you can observe above, the minimum FOS of the A-term design was only 0.26. It failed at the bushings of the upper mounts but also on the turnbuckles as they can be seen in red. At this point we weren't even analyzing the mounts with the impulse loads.

Several alternative designs were created in order to achieve a better factor of safety. Some of these approaches involved the turnbuckles being mounted at the lower points of the mount, others involved moving the mounting points on the mounts, and others involved adding a third support structure to the mounts. Some of these failed designs can be seen below:

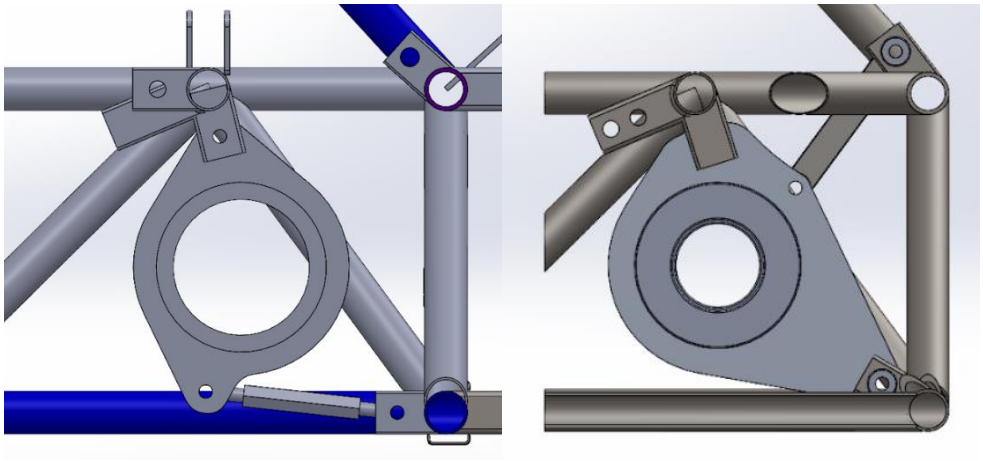

*Figure 43: Different Mounting Solutions that Were Explored*

Although they were not successful, the team was able to gain knowledge from every failed design. It became evident that adding more lateral support with the mount would decrease the bending load on the turnbuckles and that the ideal mounting configuration would be symmetrical and would distribute the load across the turnbuckle and lower mount evenly.

The big issue that we tried to avoid up to this point was changing our initial choice of rod ends. Because of the limited availability of rod ends that have both left- and right-hand configurations, the team was dreading looking for new ones. Nonetheless, after through research, we managed to find a different design of turnbuckle that could be purchased with a larger shank thread size. By increasing the size from an M8 rod end (0.315”) to a ½” turnbuckle there were significant increases in FOS. After redesigning the mount for the new turnbuckle design, we began approaching more promising FOS values:

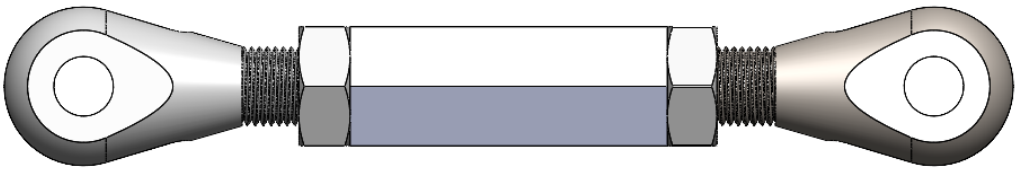

*Figure 44: Final Turnbuckle Design with ½“ Shank Size*

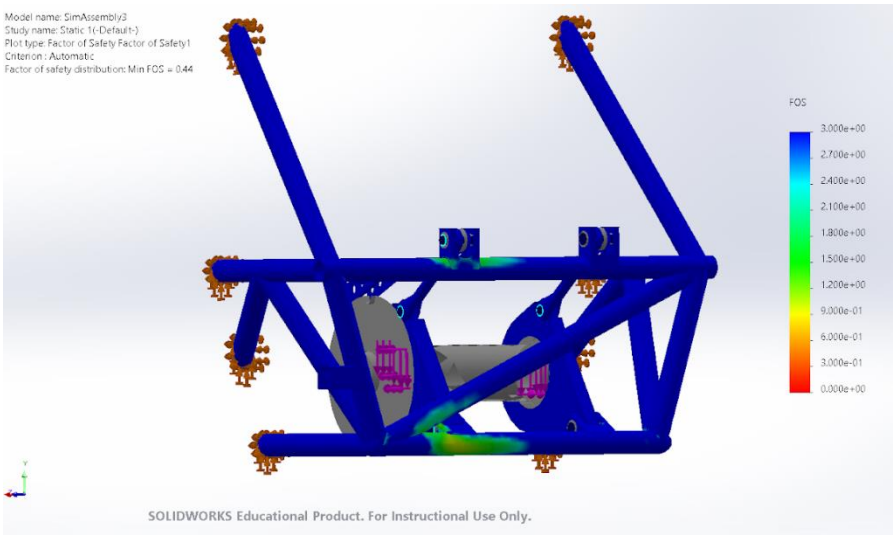


*Figure 45: FEA Analysis of New Turnbuckles and Adjusted Mounts*

The new problem that resulted from a more robust turnbuckle was the deformation to the frame. To fix this issue, a new frame member had to be added which resulted in the following:

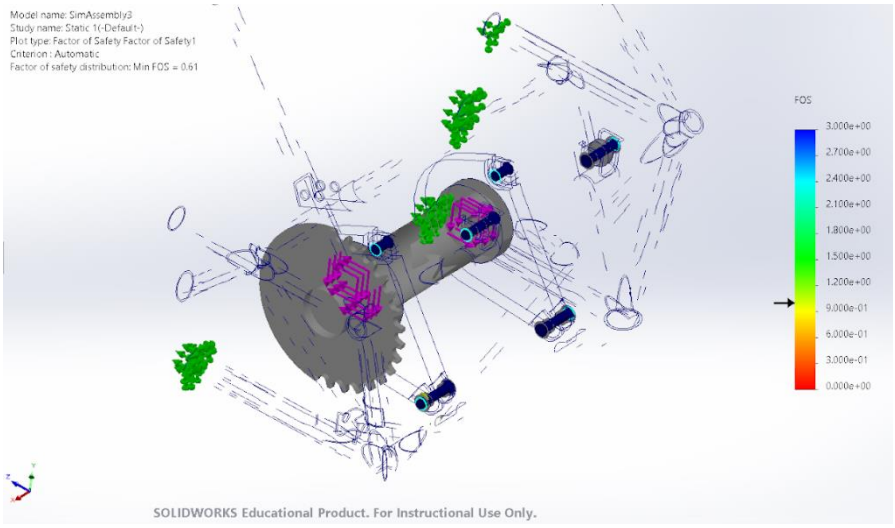


*Figure 46: ISO Clipping of FOS < 1 with New Frame Members*

Nonetheless, the material we had selected to create the frame tabs from is not available from any supplier. Consequently, the team decided to opt for flat tabs with gussets for support. This change allowed us to create larger support surfaces for the differential mounts.

As can be seen below, we were then able to obtain a FOS of 0.9 but the minimum FOS occurs at two very small stress concentration points. If we exclude these two points the FOS increases to 1.11. The results were good enough that one of the additional frame members could be removed:

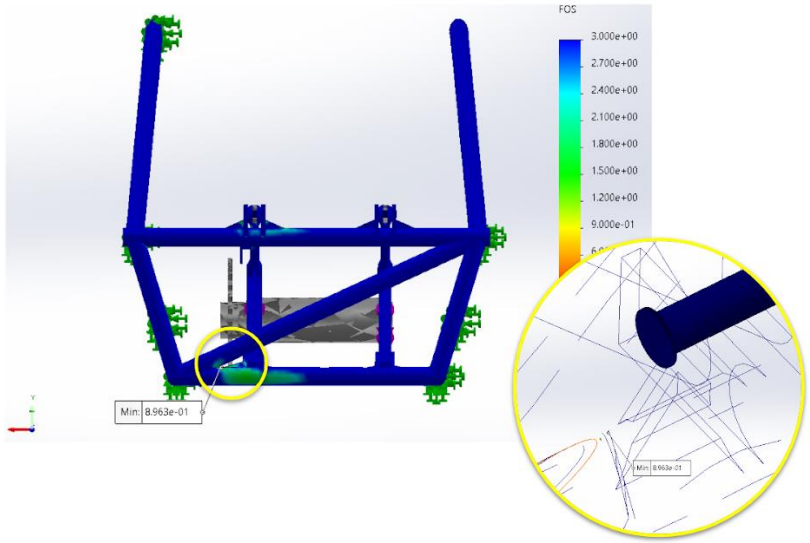


*Figure 47: Final FEA Analysis of Finished Mount*

The last step was to conduct weight savings to the mounts and add the abutment to retain the differential bearings.

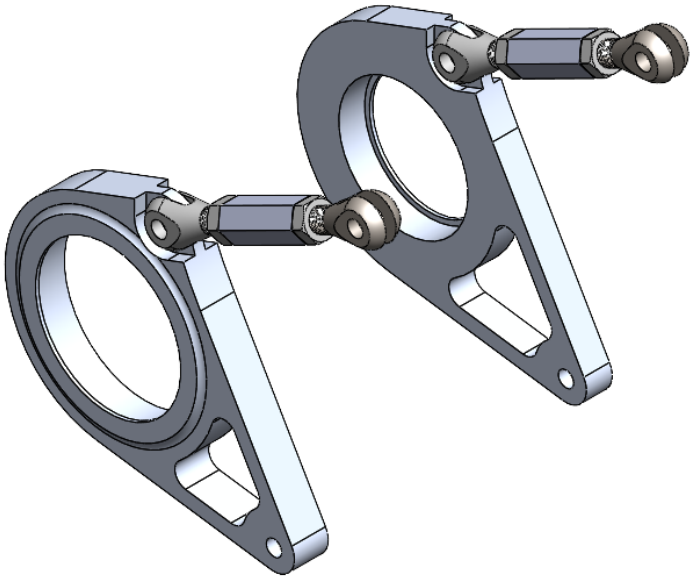

*Figure 48: Rough Final Design for Differential Mounts*

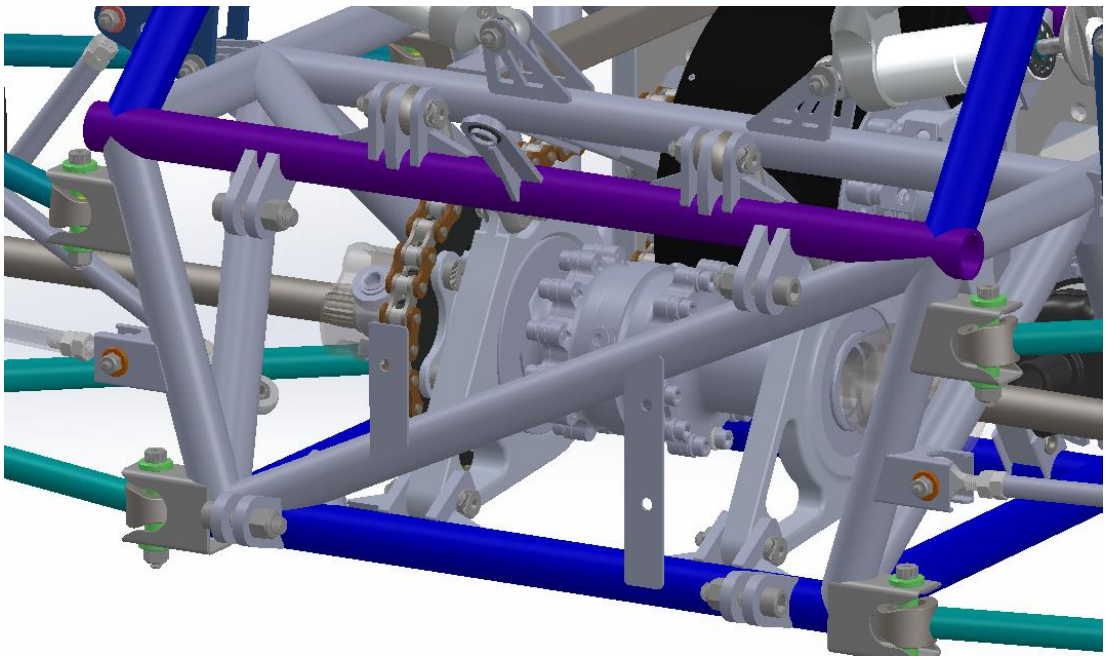

*Figure 49: Final Diff Assembly with Frame Tabs*

## Driven Sprocket and Carrier

After finishing the design for the differential mount we decided to verify the design one last time before manufacturing it. During this review we encountered a critical flaw in the design. The length of the chain required to cover both the driven and driving sprockets would not be possible due to the size of the links. If we were to manufacture the design with no changes the chain would always be loose.

The team decided to switch the sprocket to a smaller one which would keep our gear ratio fairly the same (2.14:1 instead of 2.3:1). Another benefit of this sprocket would be the bigger clearance to the required scatter shield since in the previous configuration we only had about 1/16” to ⅛” of clearance. As such, we decided to go for the JTR1478 30 teeth sprocket, no model was available for this product so once we received it, we proceeded to model it in SolidWorks.

*Figure 50: JTR1478 30 Teeth Sprocket in SolidWorks*

With the sprocket modeled in SolidWorks, we could now use it to design the sprocket carrier. The three biggest considerations when designing the carrier were ensuring the driven and the driving sprocket were aligned, ensuring good clearance with all differential components, and trying to minimize its weight.

The first iteration of the sprocket carrier design can be seen below. The design was made with manufacturing in mind and the team planned to use EDM to cut the splines in the inside of the part.

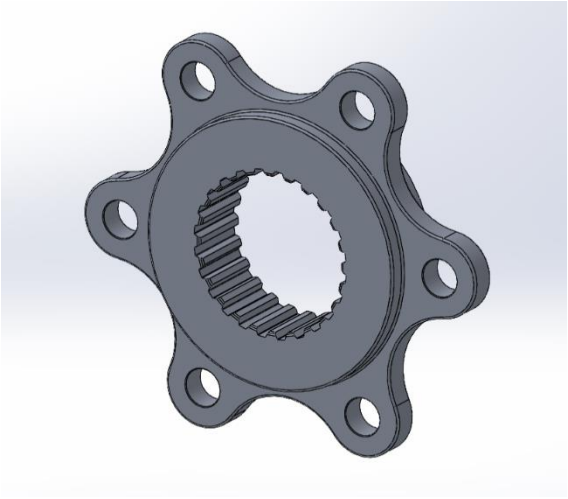

*Figure 51: Sprocket Carrier Model Showing Splines*

Another idea we had was to make the carrier a little bit smaller than the size required in the model. This is because the welding is not 100% accurate to the model and we wanted to ensure that the two sprockets would be inline. With the help of spacers we could more finely position the sprocket in the car while still allowing for testing. The plan is to, in the future, re-manufacture the carrier to the exact size required. This can be seen in the figure below.

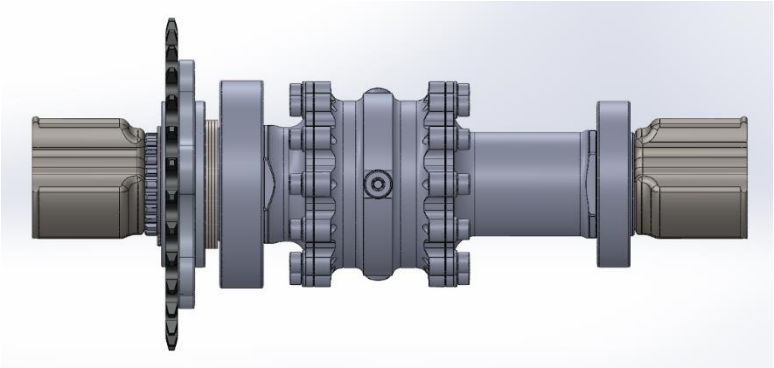

*Figure 52: Model of Sprocket and Carrier with Shims*

The next step was to verify that the sprocket and the carrier would be able to withstand the high torque of the electric motor. The first challenge was to determine what the confidential alloy used for the JTR sprocket was and its properties. After reading multiple forums it was able to determine it had properties very similar to *SAE-AISI 1049 (G10490) Carbon Steel*. We then set up the static simulation with forces meant to simulate the impulse that the parts would experience in the same fashion as the differential and motor mounts. The results were very promising, showing a minimum FOS of 2.5 even while experiencing impulse loads.

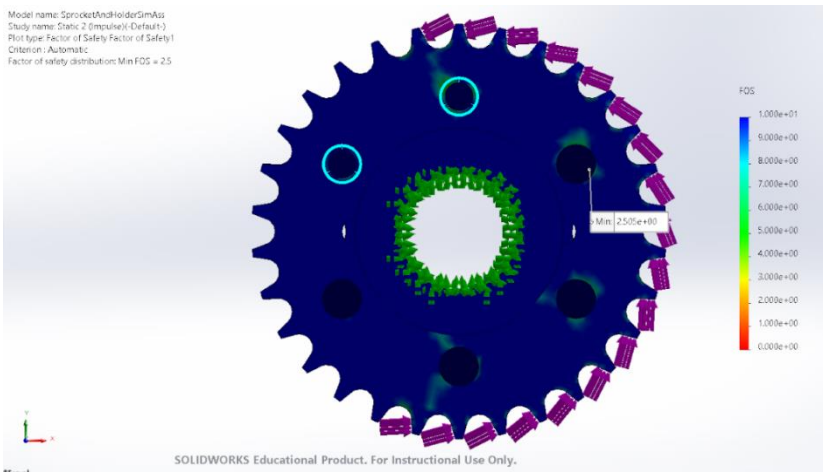


*Figure 53: FEA of Sprocket and Sprocket Carrier Under Impulse Loads*

The parts were then manufactured and installed into our differential assembly. We were also able to ensure the sprockets were aligned by installing the entire differential assembly onto the car. Both the final parts and the installed components in the car can be seen in the figures below.

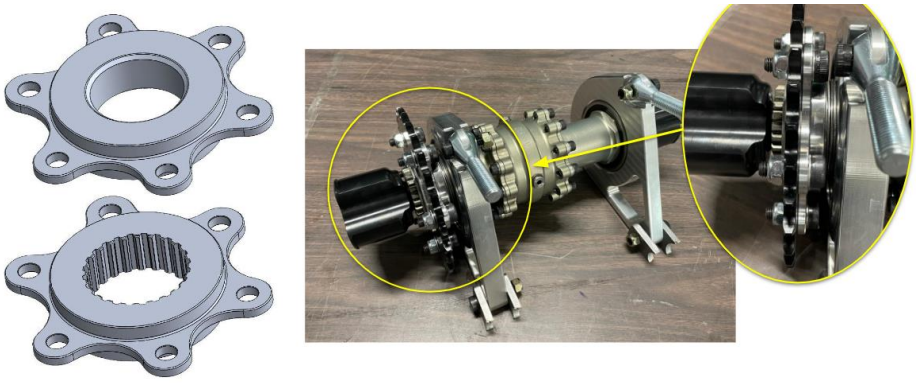

*Figure 54: Sprocket and Carrier Model and Final Assembly*

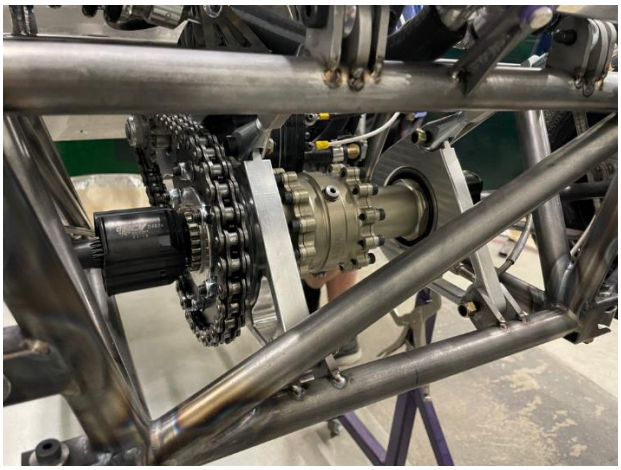

*Figure 55: Differential Assembly Mounted on Frame Missing Gussets*

## Motor Mounting Strategy

The creation of a new motor mounting strategy necessitated extensive modeling iteration and FEA analysis. While this year's competition team utilized the same EMRAX 228 as was used in previous years, our new Tractive System delivers more power than was previously attainable (EMRAX 2024). In order to ensure that the motor mount will survive both this increased potential impulse and harmonic failures, the team decided to utilize an FEA study including a maximum torque event while cornering at 3g with an applied force placed on a representative sprocket tooth face on an improved dummy motor and 6061 T6 aluminum motor mounts. Initial studies utilized a calculated force of 6,969.7 N, but upon working with our advisors to effectively study impulse loads, that force was doubled and added to the assembly. Seen in the following image is the FEA study setup that was used:

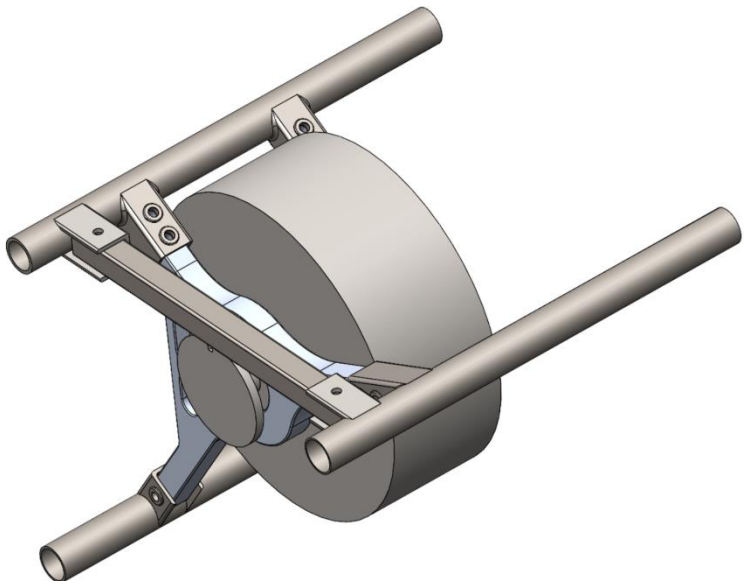

*Figure 56: Motor Mount FEA Model*

The cut-down frame seen above was created through the addition of assembly cut features in order to negative unrepresentative stress concentrations at infinitely thin portions of the unwelded frame model. Additionally, a representative “dummy motor” was created in order to simplify the study’s

mesh and it is treated as fully rigid. The following figures provide further detail regarding the application of our impulse load and the gravity setup used to simulate cornering forces:

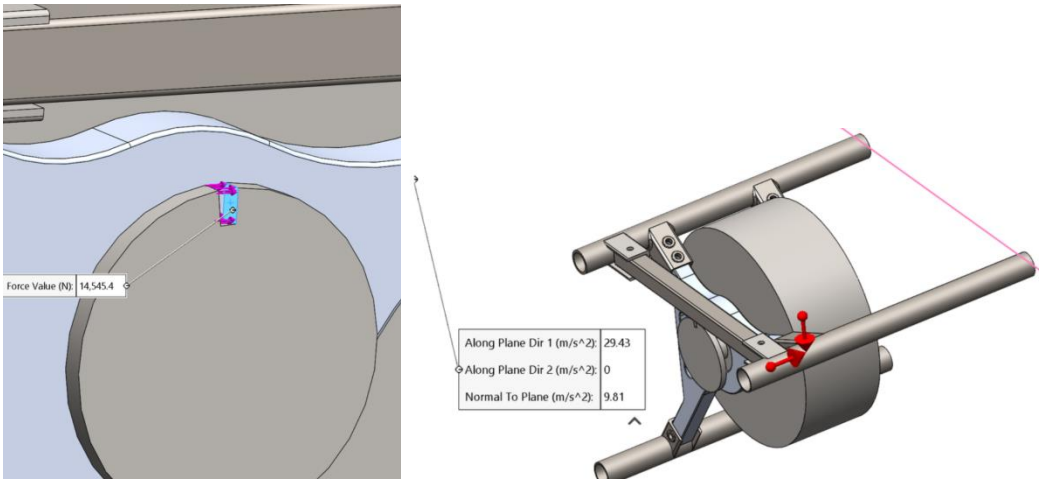


*Figure 57: Motor Mount FEA Load Setup*

Ultimately, our improved design yielded a satisfactory minimum Factor of Safety:

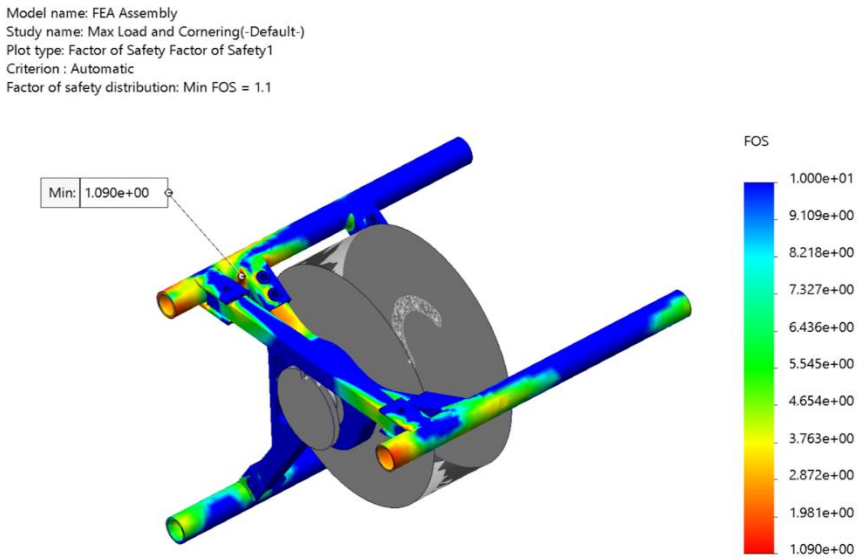


*Figure 58: Motor Mount FEA Result*

While that min. FOS is comparatively low, it is important to note that the team believes that such a load case, particularly as an impulse load, is highly unlikely. In addition to passing a static-load FEA study, the group conducted a resonant frequency study, the results of which are as follows:

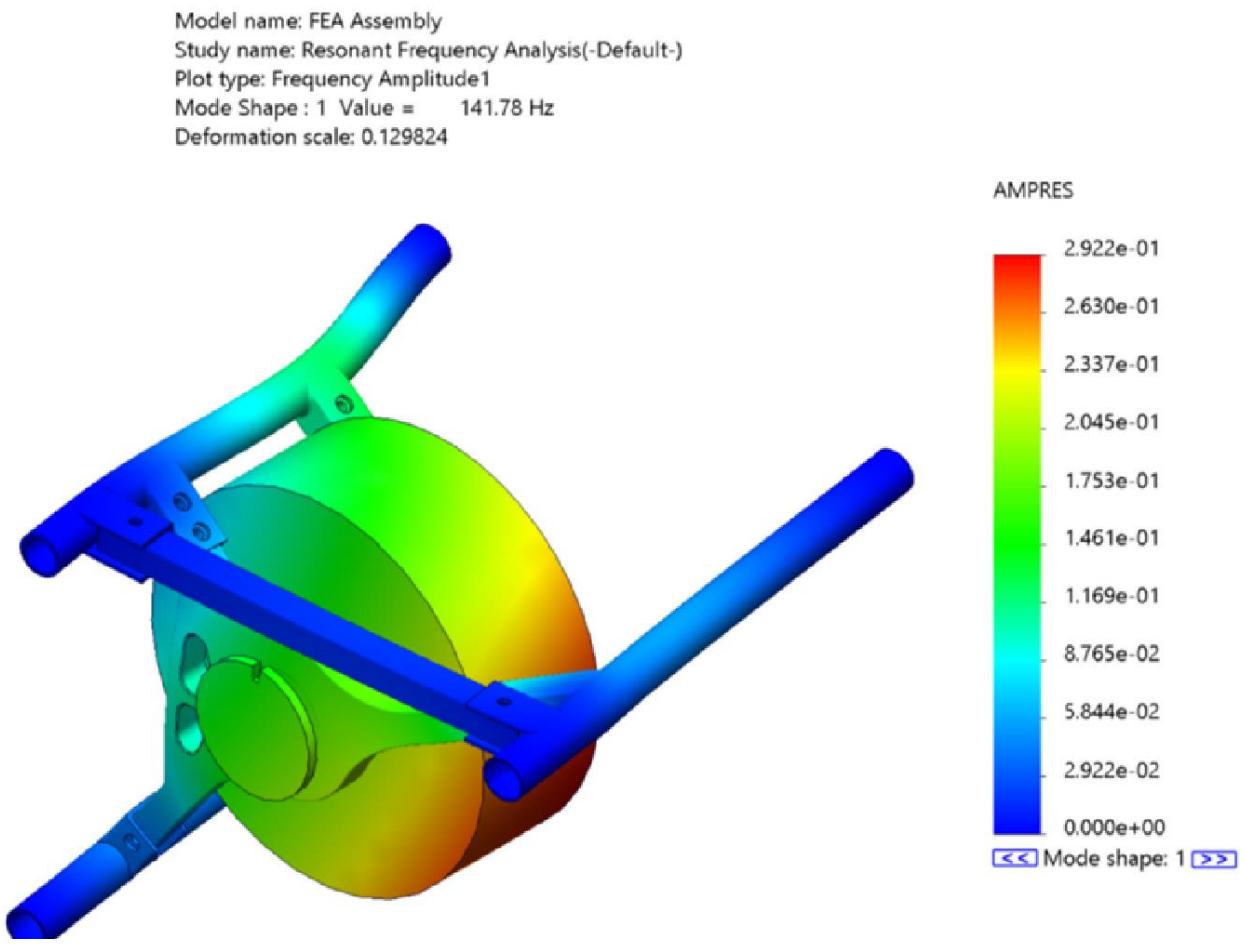


*Figure 59: Motor Mount Resonant FEA Result*

The above study confirmed that the first problematic load frequency occurs at frequencies higher than 141.78 Hz. Given that the maximum rotational speed that the EMRAX 228 can achieve is 6,500 RPM or 108.33 Hz, the team contends that our assembly will be able to operate safely from a resonant-frequency perspective. With the design verified, it is important to document the exact specifications of the parts that the team designed in order to successfully create a robust assembly. Selected information is included in the following sections.

## Three-Arm Motor Mount

As seen in the preceding figures, the sprocket-side motor mount necessitated the addition of a third mounting location, integrated as follows.

*Figure 60: Three-Arm Motor Mount*

This arm was added to increase the structural rigidity of the mount under the most stress. Additionally, it is important to note that the top two arms are now designed to employ two ¼-20 Grade 8 bolts assembled in dual shear. This design choice was critical in improving the ability of our 4130 welded frame tabs to survive the extreme load case that our motor can produce.

An additional note on part creation is of crucial importance. A decision that was made early to round several angular measurements led to minor part misalignment. As such, the base sketch of both motor mounts were replaced by the following sketch that used exact reference to our frame design.

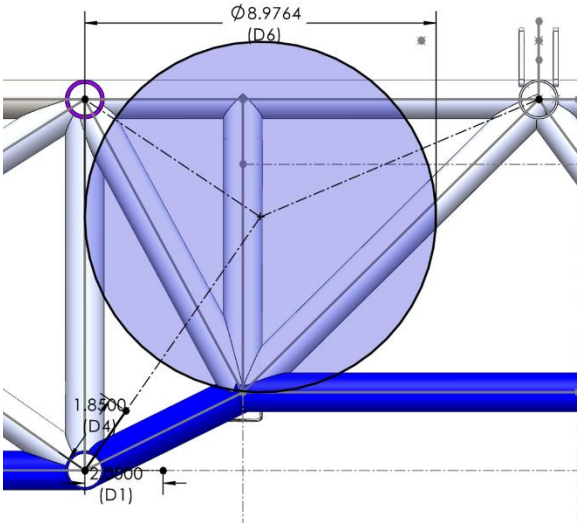


*Figure 61: Motor Mount Base Sketch*

The dimensions included in this sketch were crucial in ensuring that the profile of our mounts matched and that they would allow the motor to be fully encompassed by the envelope of the frame. The above figure also displays our desire to fully contain the motor within the static frame envelope to negative the addition of a subfloor/skid plate.

Finally, 4130A steel top-hat spacers were required to ensure proper part fitment as ease of assembly, a representative example of which can be seen below. The addition of a bolt-in 4130 box section was also required to pass FEA

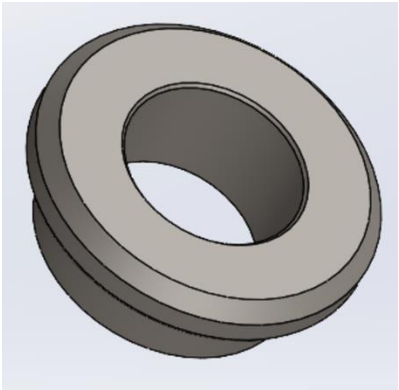

*Figure 62: Motor Mount Top-Hat Spacer*

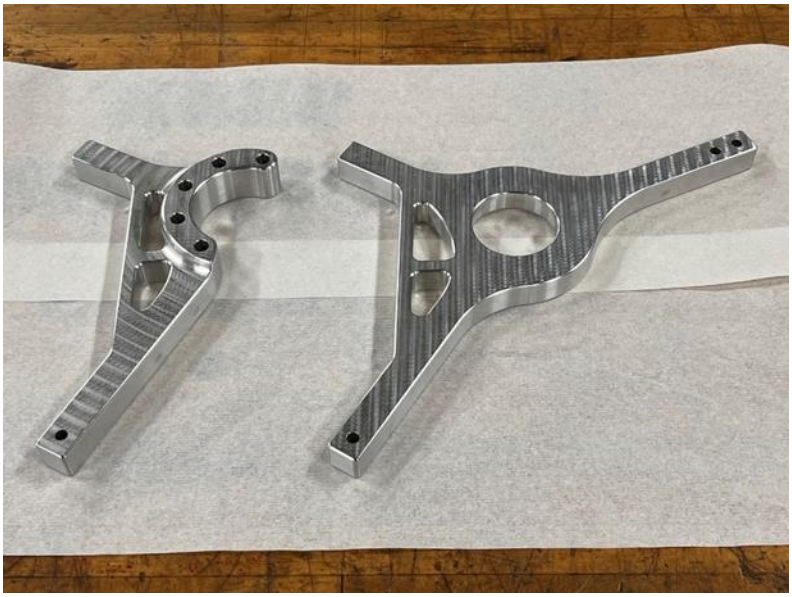

*Figure 63: Manufactured Motor Mounts*

## Motor Cooling

Using the radiator taken off EV23 would allow the team to reduce costs and use a component that has proved its reliability and effectiveness. The radiator has a 7.91" x 12" core that is manufactured by Mishimoto for a 2001-2005 Yamaha YFM660 Raptor ATV. To further validate its effectiveness at cooling our components, the Raptor has a 26.8 kW engine, assuming a 30% loss of energy from heat transferred to the radiator, the cooling system on the Raptor is beyond capable of cooling a 8.92 kW system. The EV24 motor operates at a max power of 100 kW and around 28 kW of continuous power.

$$\text{Max power dissipated} = (\rho_{max}/\eta_{motor})-\rho_{max} = (100\text{ kW}/0.92)-100\text{ kW} = 8.70\text{ kW}$$

$$\text{Continuous power dissipated} = (\rho_{continuous}/\eta_{motor})-\rho_{continuous} = (28\text{ kW}/0.92)-28\text{ kW} = 2.43\text{ kW}$$

When the motor is operating at max power, the radiator is equipped to handle the cooling load and when the motor is operating at continuous power, a more realistic case when the car is being operated, the radiator is beyond capable of cooling it. The motor controller must also be cooled,

the manufacturer suggests a flow rate of 10l/min. Our pump can achieve 25 l/min @ 1.40bar and 40 l/min @ 0.80bar. These specifications of both our pump and radiator validate the cooling capacity of EV24.

Radiator mounting was achieved by waterjet tabs welded to frame members in which a cross bar will be inserted through the radiator tabs and through bolts will hold the cross member to the tabs. The lower tab will incorporate a hole in which the existing mounting pin on the radiator will slide through. All interfaces will include rubber grommets to reduce noise and vibration between components. Finally, an off the shelf, rules compliant catch can was specced, reverse engineered, and mounts were designed.

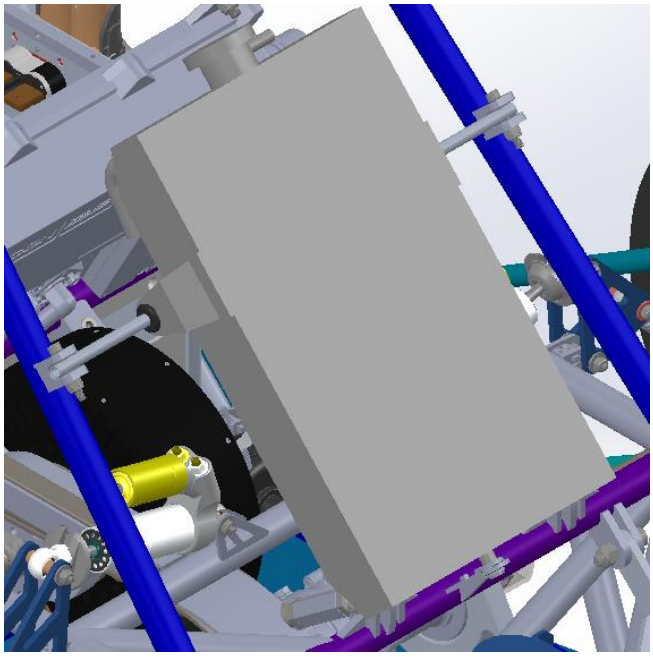

*Figure 64: Radiator Mounted in CAD*

## Scatter Shield

An incidental benefit of the aforementioned bolt-in 4130 box section, is that it serves as a perfect mounting location for a rapidly removable and rules compliant scatter shield. Said component is heavily regulated and we have to follow the competition rules for minimum thickness, width, and its overall shape. The final drivetrain shield must cover the chain from the drive sprocket to the driven sprocket while starting and ending parallel to the lowest point of the chain.

With this rule, the design of the scatter shield was mostly straightforward thanks to the design of the differential mount and the chosen size for out driven sprocket. In the sketch below you can see the position of the fixed driven sprocket and both extreme positions for the continuously adjustable.

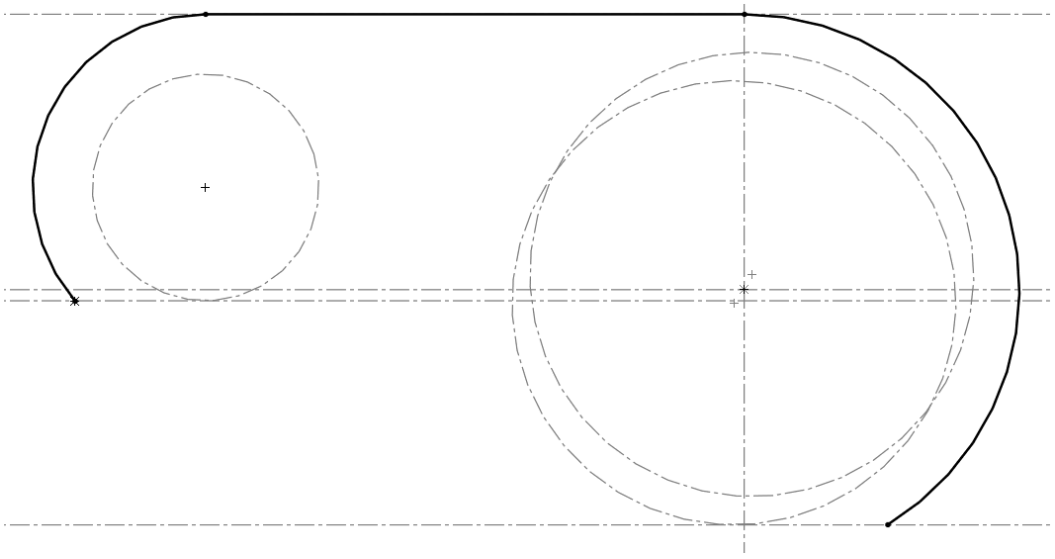

*Figure 65: Base Sketch for Scatter Shield*

The sketch was then extruded using the sheet metal feature in SolidWorks but clearance holes were needed for drivetrain components. The team had to submit a rules ticket about the cutouts since it meant that the scatter shield was not three times the thickness of the chain. We were told it

wouldn’t be an issue as long as we ensured that our clearances to the drivetrain components were tight. We then designed these cutouts to have a clearance of just 1/16” to the motor and diff. mount.

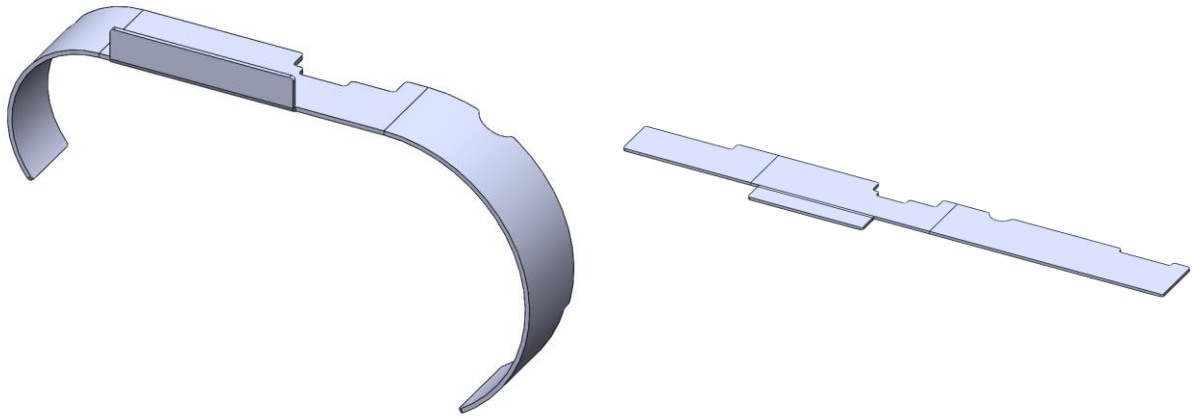

*Figure 66: Scatter Shield Modelled Using SolidWorks Sheetmetal*

The scatter shield was then manufactured with a … sheet of … on a waterjet. The flat sheet metal was then bent to the required radii. As mentioned before, the mounting strategy revolved around welding the scatter shield to the bolt-in 4130 box section member for quick removal.

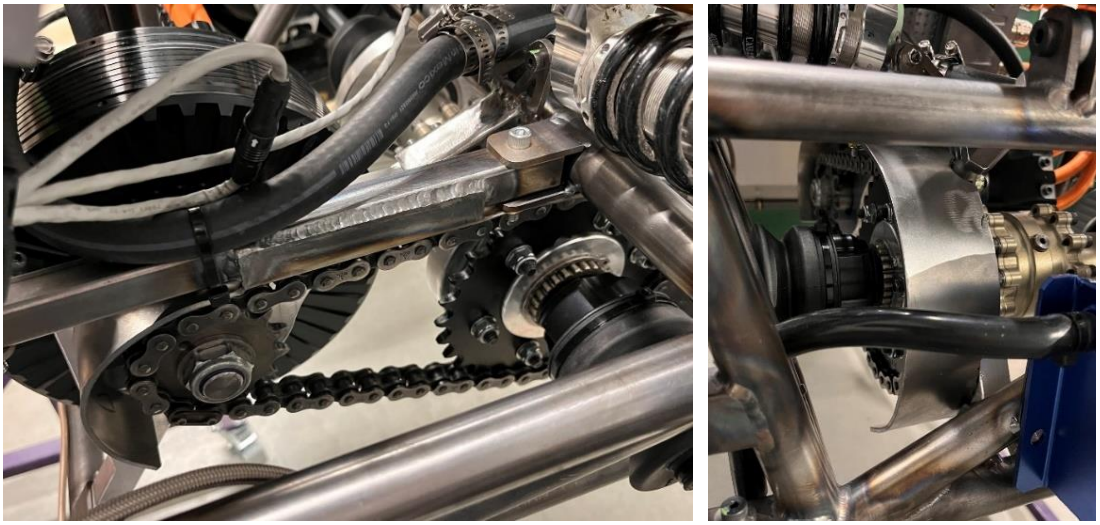

*Figure 67: Scatter Shield Installed in Car*

# Steering

The steering design for EV24 consists of a 120° gearbox with 60° angled miter gears. This gearbox design will be the best option for the car. We originally designed the car around a straight shaft steering design which is easy to manufacture and will not increase steering effort through the use of universal joints or gears. After mocking up this design in the car, we quickly realized that this will not be a safe or comfortable design for our larger drivers. After that realization, we gravitated towards a double universal joint setup. This would have been more difficult to properly constrain and make rules compliant for the cockpit template.

This gearbox design will house both gears and will be supported by thrust bearings and tapered roller bearings. It will consist of an aluminum body with carbon fiber finger guards.

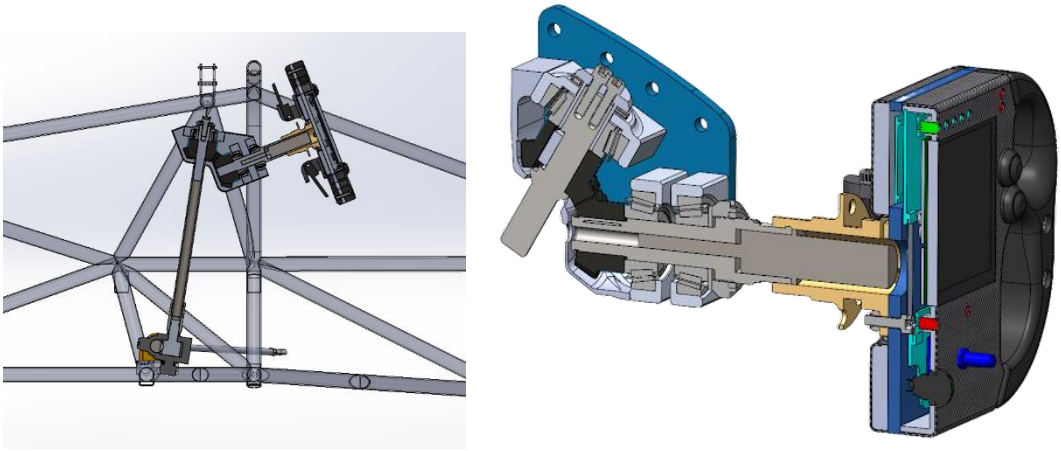

*Figure 68: Steering Assembly Overview*

# Bodywork

The aerodynamic goal of EV24 was to reintroduce aerodynamic design and composite manufacturing to the team. Our requirements were to maximize downforce while maintaining low overall drag, so we chose not to build a front or rear wing. Our scope for this year included the car's underbody, diffuser, nose cone, and side panels.

The choice of what components we were going to design was based on prior art that indicated that a large percentage of a car's downforce is generated via ground effect (Katz, 2006).

## Nosecone

The team wanted to manufacture the car's nosecone early in the year. This is normally a task that can be delayed to the late stages of manufacturing as it is not critical to the functioning of the car. Nevertheless, manufacturing the nosecone early in the year gave us more time to understand and improve our skills with composites as well as the opportunity to adjust throughout the year.

The design of the bodywork began with the nosecone as it is the only required component. When it comes to designing the nosecone there is only one rule that is worth mentioning is that "the nose must have forward facing radii of at least 38 mm".

Unlike previous years, where the team went with a lowered tip nosecone design, the approach this time was a raised nosecone. Both designs have their upsides and downsides but as we were interested in designing a floor for the car this year we went for the latter concept. This is because a raised nosecone allows for better airflow under the vehicle which improves the performance of the cars undertray and diffuser (OGAWA et al., 2009).

Designing the nosecone involved the use of lofted surfaces in SolidWorks. There was a lot of learning while making the design which meant that the team created several iterations. The first of which you can see below:

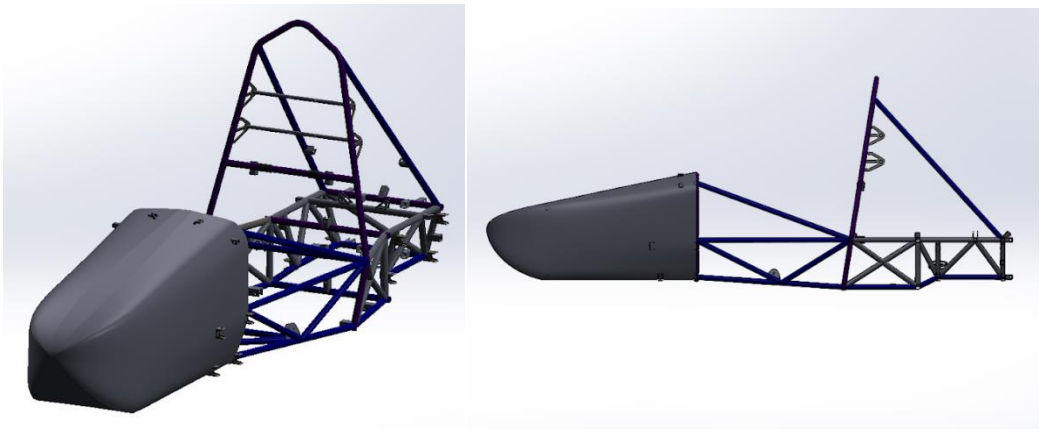

*Figure 69: First Nosecone Iteration*

As seen in the figure above, the bulk edge of the nosecone is raised high to allow for airflow under the vehicle. This is a trait that is consistent through all iterations. The problem that the team had with this design was the uneven profile of the nosecone and the fact that all edges converged at the very tip. The second design aimed to fix these issues.

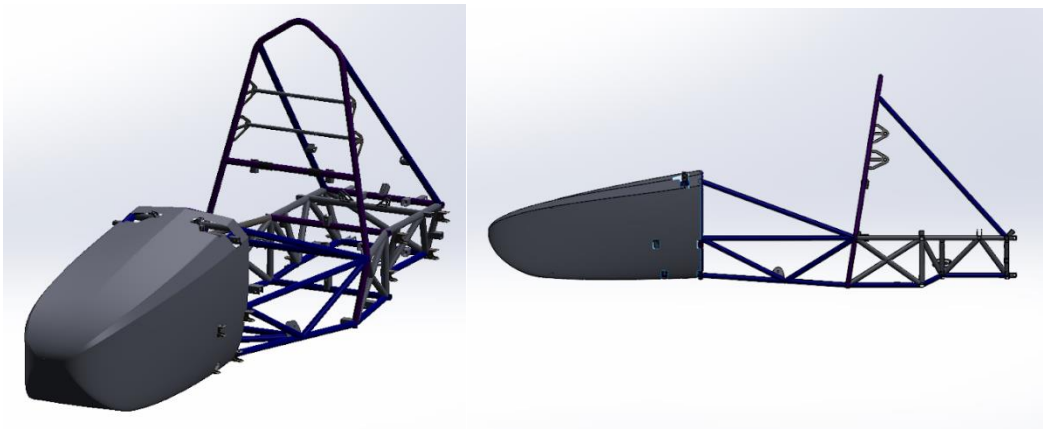

*Figure 70: Second Nosecone Iteration with Flat Tip*

As it is evident in the image above, the nosecone no longer has a single point where all edges converge, and the cross section of the design is smoother. Nonetheless, the front of the nosecone

is a completely flat surface which would create a stagnation point. The improvements for the next design would be to have a curved bulk edge.

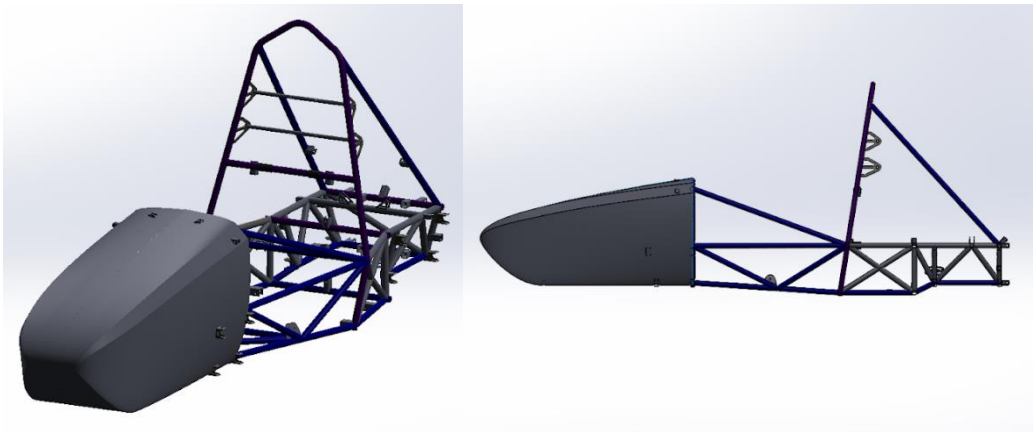

*Figure 71: Final Nosecone Design*

The last design consists of multiple lofted surfaces that were knitted together. This allowed for more control over the surface geometry when creating the surface lofts. The team also preferred this design in terms of aesthetics.

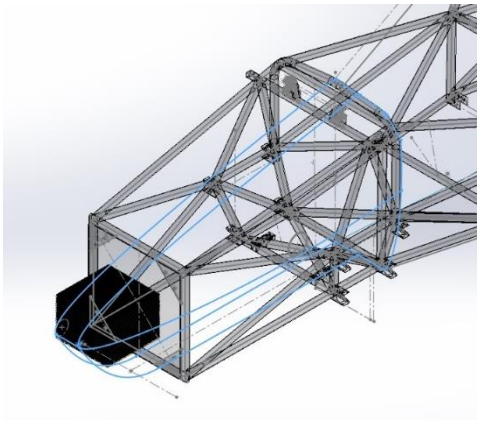

*Figure 72: Sketches Used to Create Nosecone*

Nosecone manufacturing has come with many lessons throughout this process. The steps that were followed were manufacturing of the plug with a CNC router, assembling the foam slices together, preparing the plug, applying mold release, and finally doing the carbon fiber layup.

Brenner Signs, a sign shop located in Plymouth, MA has let us use their 5’x10’ CNC router. This has increased efficiency when cutting each foam slice.


*Figure 73: Initial Plug Manufacturing Operation*

All machining was done with a ½” endmill which was used to do a 3D adaptive roughing pass over each piece. On future bodywork machining we will be using a ½” ball endmill for a 3D finishing pass. This will give more accurate results and have less finish sanding.

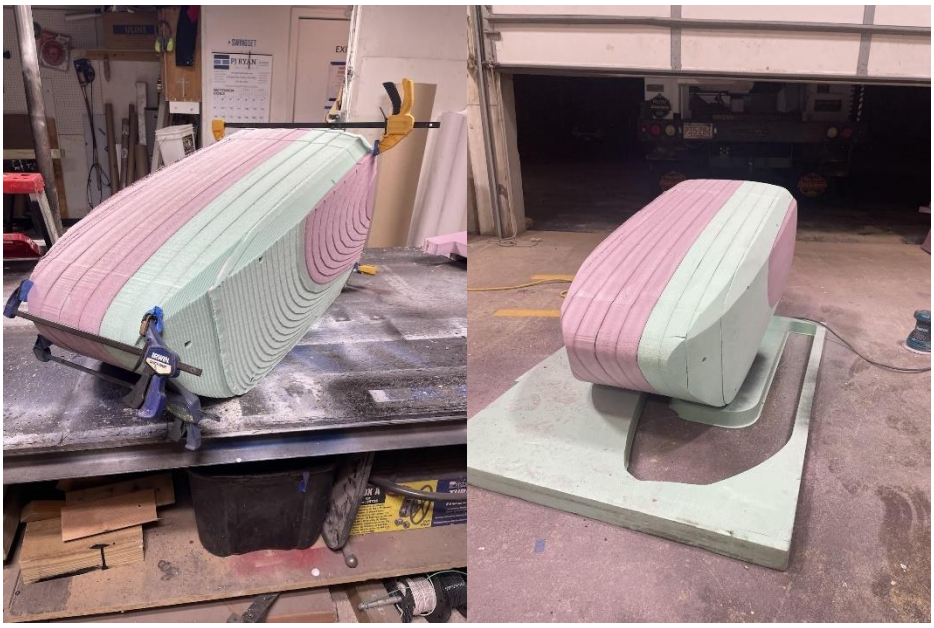

*Figure 74: Nosecone Plug Assembly*

After the sanding is finished, the next step is to prep it with mold release. To ensure a smooth surface for the carbon this takes a couple layers of mod podge as a barrier, paint, mold release wax, and PVA spray solution. It was learned through this process that Bondo melts this type of foam. This was a major setback in the nosecone process but was fixed with wall spackle which does not melt. Once the plug was prepped, it was waxed and sprayed with PVA.

*Figure 75: Nosecone Plug Preparation*

After mold release has dried, the plug is ready for the layup. The nosecone will be 3 layers of carbon fiber. Currently, 2 layers have been completed. Some small finish work must occur to ensure a smooth look with no imperfections on the final layup.

*Figure 76: Carbon Fiber Application*

One additional layer of carbon fiber was added onto the nosecone after all imperfections were sanded out. The final layer of carbon was tinted with blue mica powder to give the nosecone a shimmer in the light.

*Figure 77: Nosecone Manufacturing Result*

Vinyl stencils were used to accurately measure out hole locations. These templates were generated directly from solidworks and allow for perfect fitment. A vibrating multi tool was used to precisely cut out all of the holes.

*Figure 78: Vinyl Cut Stencil*

## Side Panels

The side panels were designed to be foam core with carbon fiber outer walls. This means that unlike all the other removable molds, the foam machined for the side panels remains encapsulated in the carbon fiber for the lifetime of the bodywork. The side panels are double sided parts to accommodate geometry on each side of the panel. To machine the second side of the panel, a fixture plate was machined with a matching contour and specific geometry to locate the parts on the CNC router. The foam was attached to the fixture plate with double sided tape.

*Figure 79: Foam Plugs*

The inside of the side panel was machined to contour the frame members of the car to assist with alignment of the body panel as well as aesthetics inside the cockpit. Tolerancing around the frame members was increased to allow for small misalignment of the panel when fitted to the car.

*Figure 80: Side Panel Plug Mockup*

Seen below is the fixture plate setup that allowed for a two-sided part. The fixture plate is aligned with the bottom left corner of the spoil board and the origin of the two-sided part is set based off a machined feature in the fixture plate. Double sided tape was used sparingly, as it is very strong for the foam and minimal machining forces exist when machining foam.

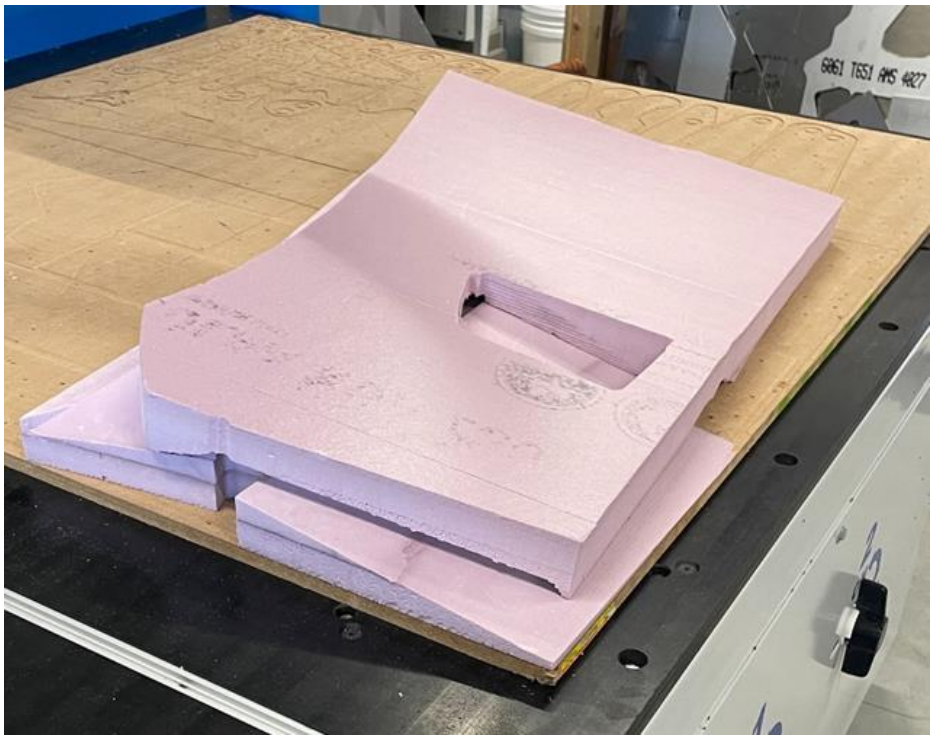


*Figure 81: Foam Plug Manufacturing Continued*

## Rear Panels

The rear panels on the car followed similar methodologies as other parts. A 3D parallel tool path was used with a flat end mill to achieve the contours of the panels. A 2D contour was used at the end of the operation to cut the outer contour and free the parts from the foam.

*Figure 82: Rear Panel Manufacturing*

The louvers designed for the car used a flat end mill with a parallel tool path as well. Stepover and step down distances were decreased to improve surface finish straight off the router, as this part was difficult to sand down smoothly due to the complex geometry and nature of the foam.

*Figure 83: Louver Plug*

## Floor and Diffuser

The first floor that was designed was a simple and flat surface that would enclose the frame of the car. This would be the alternative if the team decided to not move forward with the diffuser.

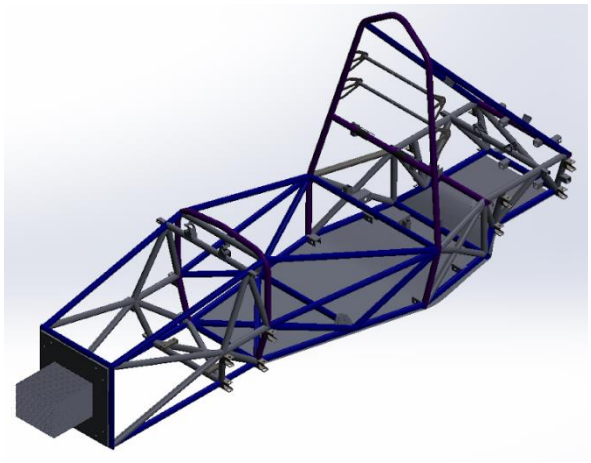

*Figure 84: First Attempt at Aerodynamic Floor*

A diffuser's optimum angle varies between 10° and 20°. With 10° being the minimum to create any significant downforce and 20° being the maximum before flow separation occurs. The problem with a 20° diffuser is that it is very sensitive to airflow and might stall if conditions are not ideal, because of this the team decided to go with 15° as it is the middle point between the two (Joseph Kratz Paper).

There is not a lot of space in the rear of the car to fit the diffuser, because of this we designed it so it would go through the jackbar. The diffuser will be tangent to the rearmost frame element and create a 15° angle with the floor. With these parameters we were able to create a cross section of the diffuser that can be seen below:

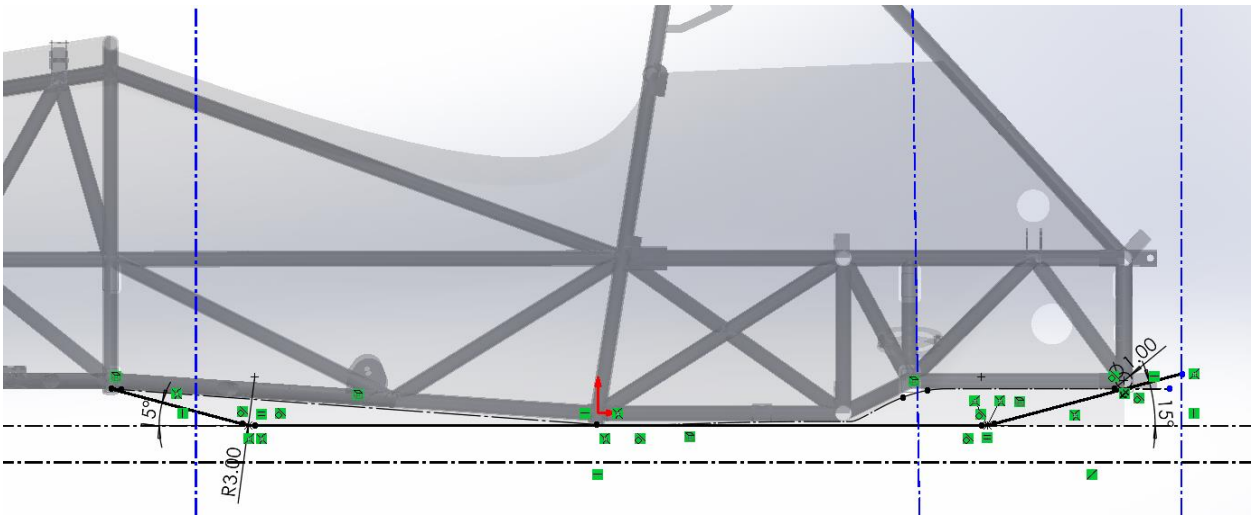


*Figure 85: Base Sketch for Floor with Diffuser*

We then extruded two surfaces, one being the cross section above, and the other a rough coke bottle shape that would be the width of the floor. These two surfaces where then cut which resulted in the floor design shown below:

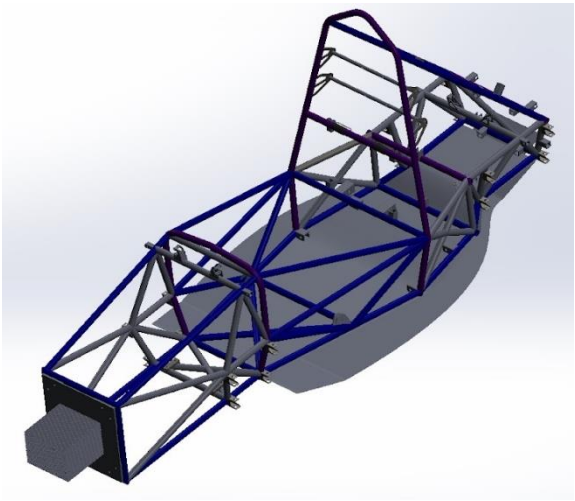

*Figure 86: Coke Bottle Floor Shape*

Nonetheless, for the floor and diffuser to work it has to be sealed. To achieve some vertical surfaces from the edge of the floor were extruded and then given a lip. In the end we had the following as out floor.

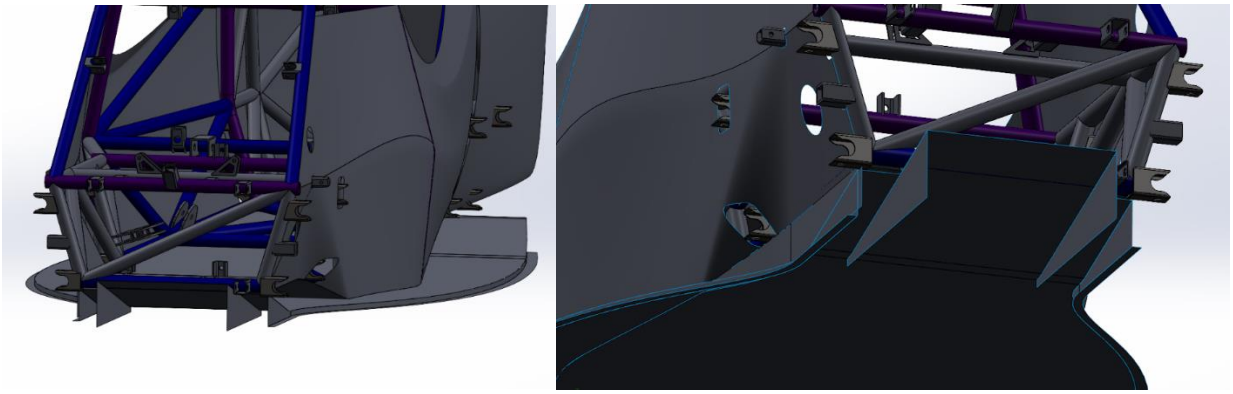

*Figure 87: First Diffuser Design*

Nonetheless, the first design had several flaws that were exposed after CFD analysis with SolidWorks fluid simulation. We were not generating any significant downforce and there was a lot of air that was able to escape from the sides of the floor. Lastly, a diffuser requires air to be compressed and then expanded but the design above allowed air to continuously expand followed by a compression which is the opposite of what we want.

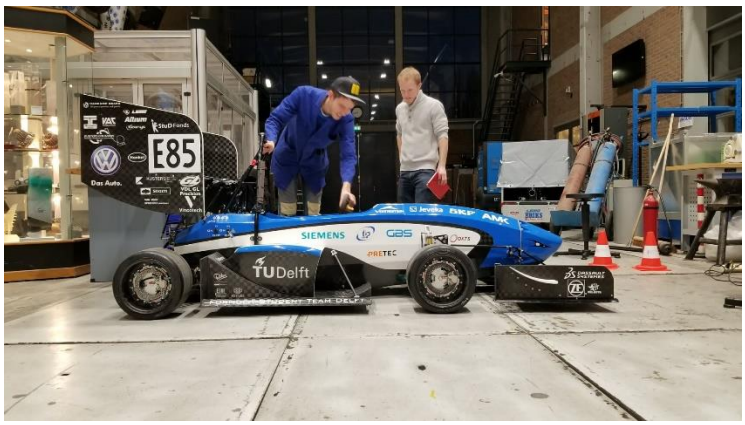


*Figure 88: Design Inspiration for New Floor*

The team begun designing a new diffuser, this time also implementing the concept of "side diffusers" that a lot of FSAE teams have adopted. After the first attempt, a lot of things were learned and we wanted to implement these into the second design. This included, respecting the no aero zones mandate by the regulations, compressing the air and expanding only at the diffuser, incorporating thicker and longer side walls to prevent airflow from escaping through the sides, and

having a wide opening at the start of the underbody to maximize air intake. With all those things in mind, we came up with the design shown below:

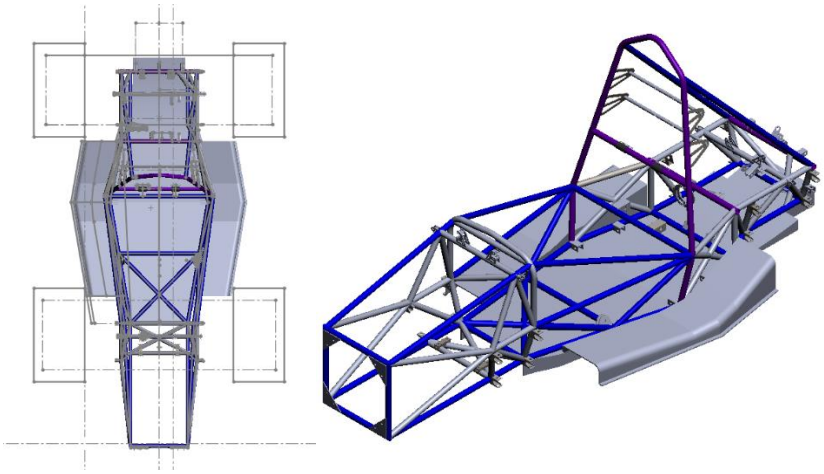

*Figure 89: Second Floor Design*

The differences are very obvious, not only did we get better at working with lofted surfaces and lofted bodies, but we also took better advantage of the geometry of the frame to constrain the air going below the car. To better understand the changes, it is good to look at the bottom of the aerodynamic floor.

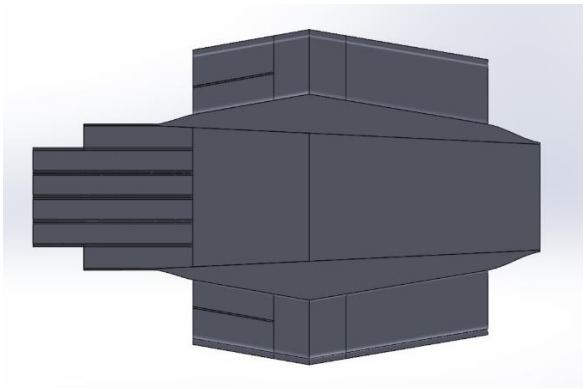

*Figure 90: Bottom View of Second Floor Design*

The team then conducted some simple CFD in SolidWorks to determine the amount of downforce that would be generated by the floor at 35 mph.

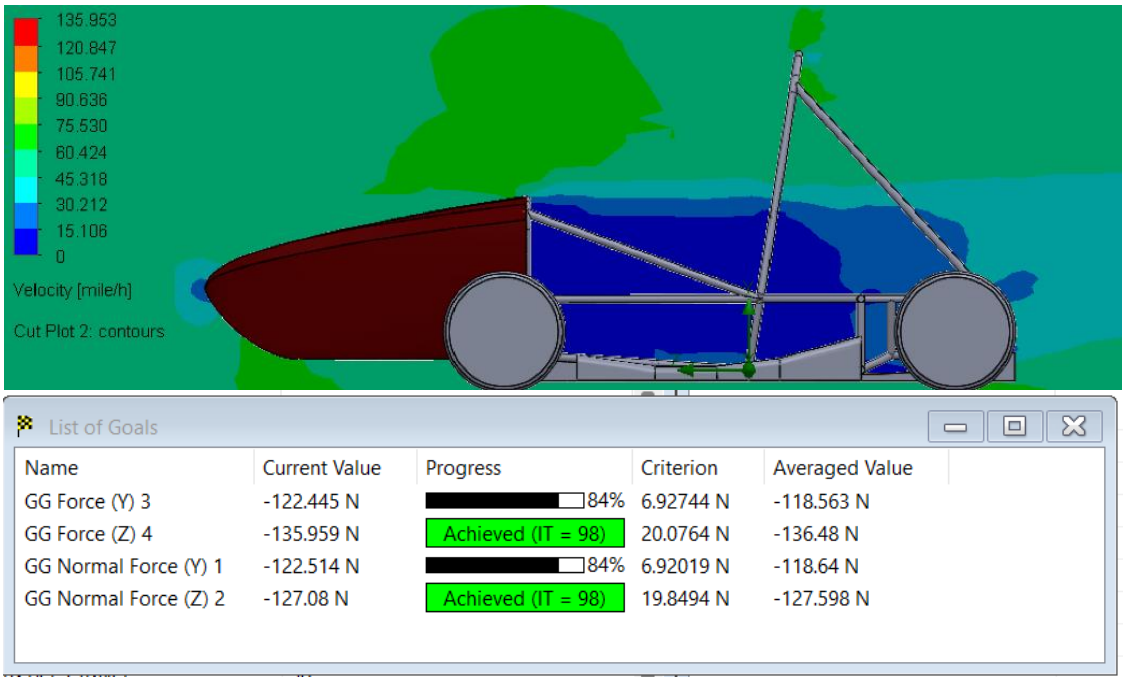


List of Goals

| Name | Current Value | Progress | Criterion | Averaged Value |
|---|---|---|---|---|
| GG Force (Y) 3 | -122.445 N | 84% | 6.92744 N | -118.563 N |
| GG Force (Z) 4 | -135.959 N | Achieved (IT = 98) | 20.0764 N | -136.48 N |
| GG Normal Force (Y) 1 | -122.514 N | 84% | 6.92019 N | -118.64 N |
| GG Normal Force (Z) 2 | -127.08 N | Achieved (IT = 98) | 19.8494 N | -127.598 N |

*Figure 91: Floor CFD Study and Results*

The study above was conducted to determine the performance of the floor but the nosecone had to be included as it affects the amount of air directed to the underbody. As it is shown above, the car is able to generate roughly 34 lbs. of downforce when moving at 35 mph. The results also indicated that the amount of downforce generated by the car's underbody and rear diffuser is almost negligible while the side diffusers are extremely effective.

In the future, it would be interesting to experiment different angles for both the front and the rear of the side diffusers. We also wanted to have experimented with the length of the side diffusers, potentially making them shorter with more aggressive angle like the car shown in our design inspiration for the new floor. Lastly, another area to look into was the implementation of flat sections near the low pressure zones, something that later research deemed necessary for optimum performance.

## Completed Bodywork

The process of arriving at full bodywork on the car followed the steps of mold manufacturing, mold preparation, carbon fiber layups, and finish work and trimming. Each step came with their own challenges and lessons. Ultimately, we were successful at bringing back full bodywork to our car.


*Figure 92: Bodywork Assembly*

# Accumulator

## Design

Our accumulator is designed to be highly modular, featuring eight individual hot-swappable segments each with its own management system. These segments combine to give our vehicle a total of 480 individually fused Lithium Ion cells.

The design philosophy of the accumulator was based on prior struggles with maintenance. To keep design complexity to a minimum the team made extensive use of OEM connectors and repeatedly practiced routine and critical maintenance tasks.

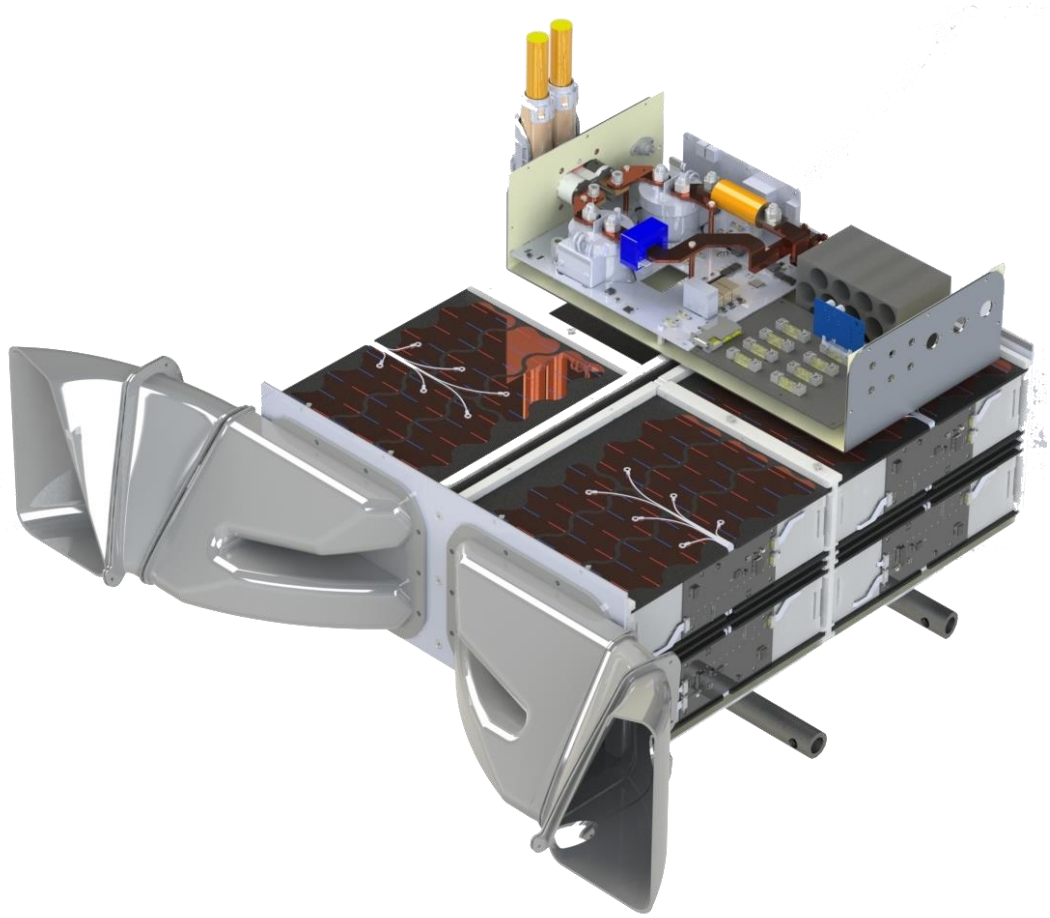

*Figure 93: Accumulator Cutaway*

## Manufacturing

The major feature of our accumulator manufacturing process was the use of an open-source spot-welder from Keenlab. This device coupled with improved internal manufacturing methodology has lead to improved performance and spot weld robustness.

## Cooling

Individual cell temperatures are monitored by 144 independent thermistors attached to our bespoke AMS. Based on that high level of monitoring coupled with prior experience, the Tractive System team determined that an entirely passive cooling solution would be most beneficial (WPI Formula SAE). The external envelope of the ducts was dictated by the geometry of the frame, firewall, and accumulator itself, optimizing the internal geometry of the ducts proved quite challenging. The initial design of the ducts, seen below, was quite unreasonably complex.

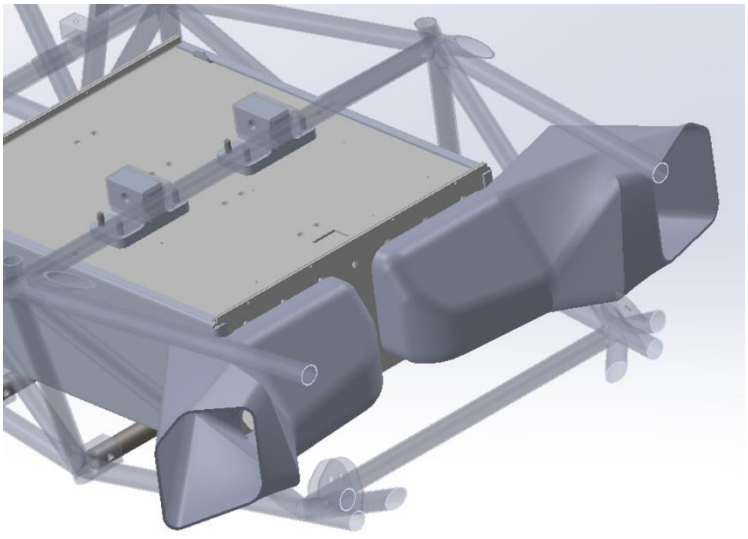

*Figure 94: Initial Cooling Duct Design*

That initial design revealed that the only feasible design would be one that envelopes the frame and is bolted to the firewall and seen in the below figure.

*Figure 95: Final Duct Design*

These internal portions of the ducts are attached to the accumulator itself by press-fit studs and mate to the external shell that envelops the frame member.

Creating the external geometry of the duct was extremely simple given the constraints in place by other components – the major challenge became internal geometry optimization.

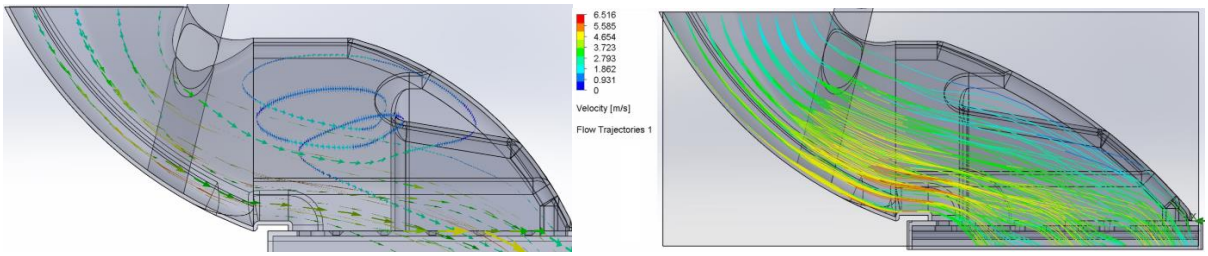


*Figure 96: Accumulator Duct CFD*

SolidWorks CFD was used to study the flow of air through each duct and into the accumulator itself. The above studies proved particularly useful – the initial design, seen above left, led to the generation of significant turbulence and poor angles of attack entering the accumulator. This study allowed to team to identify the problematic geometry and validate our adjustments.

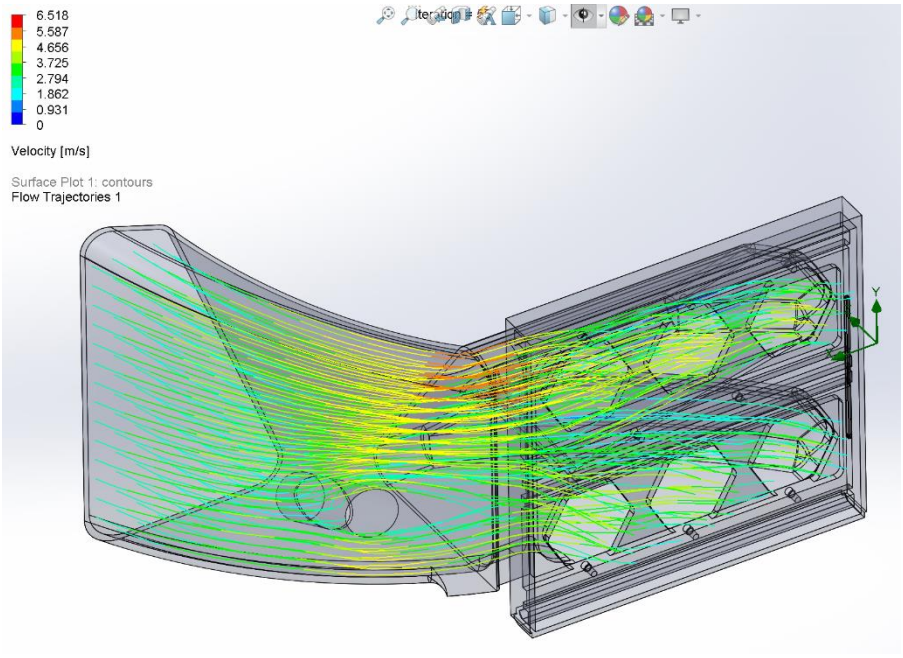


*Figure 97: Additional Accumulator Duct CFD*

With all possible theoretical validation completed, the team turned its attention to prototyping and testing the initial design. To minimize first-iteration print complexity, the duct was split into three parts, the outermost two of which were printed.

*Figure 98: Duct Prototyping*

Once some minor post-printing modifications were made, the parts were test-fitted into the vehicle. Upon doing so, several component interference instances were located. To temporarily continue the test procedure, clearance was created manually.

*Figure 99: Duct Prototype Post Modification*

Once modifications were made, the prototypes were able to successfully verify clearance with the firewall and frame as well as the alignment of bolt holes vertical faces. Sealing the duct components was accomplished by utilizing weatherproof stick-on foam. Additionally, the largest portions of the duct were used to retain our anti-material intrusion mesh.

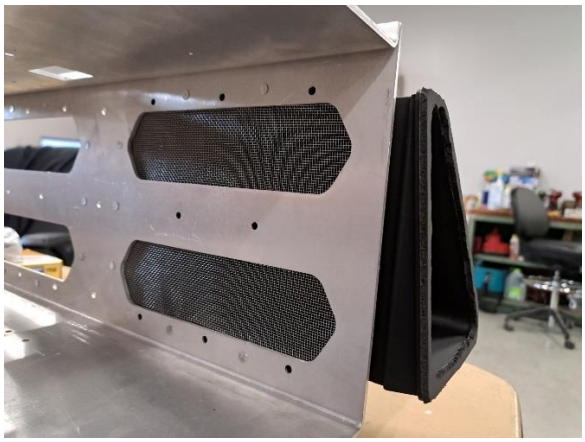

*Figure 100: Accumulator Anti-Intrusion Mesh*

The final components of the duct were manufactured using of Overture PETG on our Bambu Lab P1S 3D printer.

*Figure 101: Accumulator Duct Post Printing*

## Pump Board

Our aim was to create a Buck-converter for the Pierburg “CWA150” pump and create a PCB board design for the pump controller. The pump was supposed to take an input voltage of 22V nominal and transform it into an output voltage of 16V nominal and 16A nominal. The design includes a switching frequency of 3MHz. Below we have a picture of the final PCB design of our pump board which slots into the GLV box.

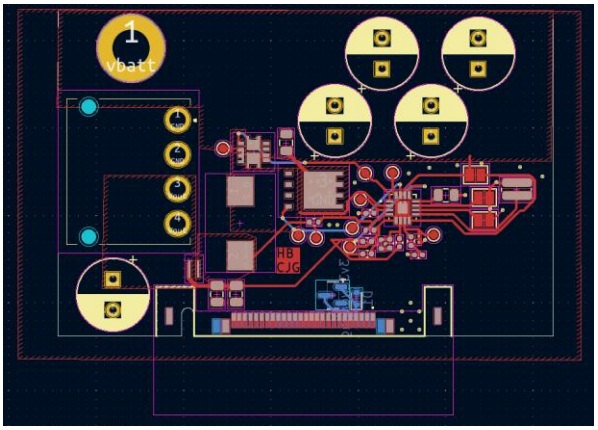


*Figure 102: Pump Board Schematic*

# Sensor Board

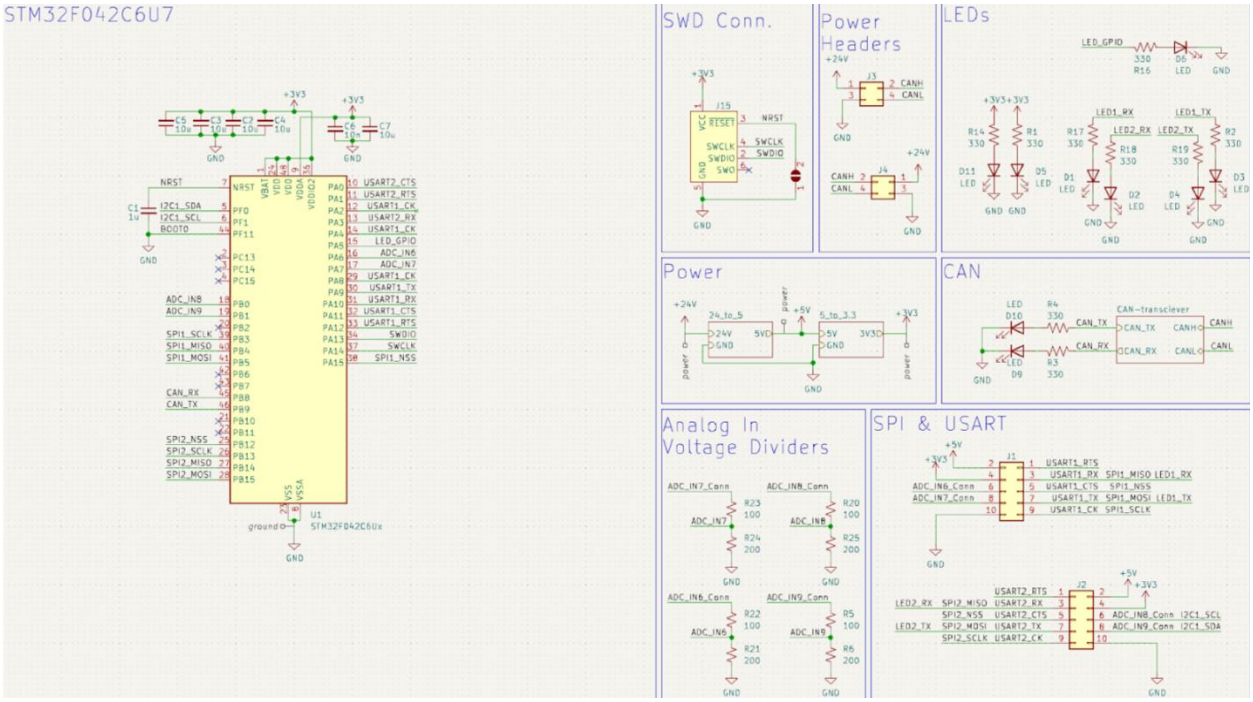


*Figure 103: Sensor Board Schematic Overview*

A primary goal this year was to improve our data collection and processing capabilities; to facilitate this, we set out to develop a single board that could collect data at 200 Hz. To ensure this board was the first, we sought to support various communication standards: I2C, SPI, and USART. Another goal was to refine the wiring harness, increasing cable commonality helping reduce potential failure points, giving us a requirement that our sensor board should easily integrate with our cable harness. Additionally, to supplement our desire for easy integration we set a requirement of the total size to be less than 1” by 1” to easily attach to our 1” frame tube with the main connector being on opposing sides for ease. These requirements led us to the STM32F04C6U7, a small-inexpensive-lightweight MCU that could power our boards. This helped us achieve a low build cost.

With our schematic complete we began work on the layout here we decided to go with a four-layer board to help us accomplish our size requirements. We opted to place the TAG connect and reset pads on a removable section to decrease the size of the board.

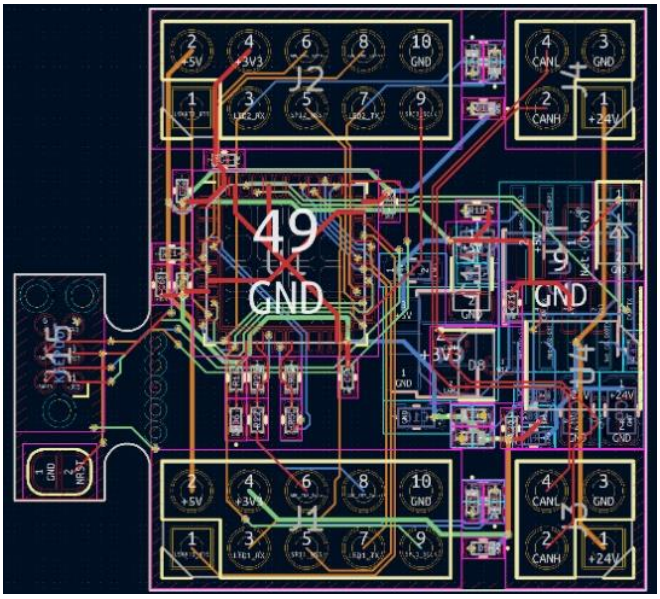


*Figure 104: Sensor Board Layout*

## Mounting

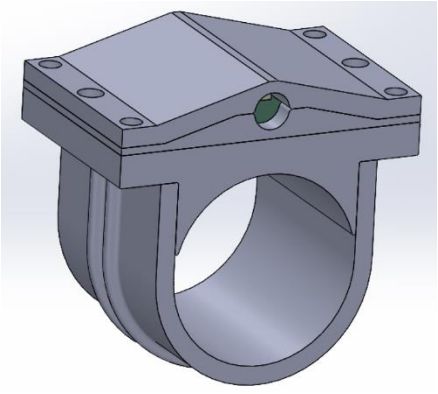

*Figure 105: Sensor Board Mount Assembly*

To mount the sensor boards, we designed this small housing mount that can magnetically clamp around the frame. There is also a hole to attach to the frame with a zip tie, with a guide around the bottom part of the clamp so that the zip tie does not move around. On the front and back of the

’house’ looking shape is a hole to clamp around a 5mm wire that will be feeding in and out of the sensor board. This clamp was designed to alleviate stress that the wires could potentially face – by clamping them on either end, the wires will not be pulled from where they are supposed to be and are therefore more secure. The bottom part of the ’house’ was designed to barely sit over the edges of the sensor board; this was purposely done so that the house would also keep the sensor board itself from moving around.

## Pedal Box

One of the applications of the Sensor Board is to read the sensor data coming from the pedal box, here we have a total of three hall sensors: two connected to our throttle, and one connected to our brake. All three of these sensors output analog data which is then digitized by a Sensor Board; the two throttle data streams are then validated; then the finalized angle measurements are relayed to the main board.

# Strain Gauge

One of the customized sensors designed is a strain gauge, a flexible PCB that measures how it stretches under stress, this was customized to fit our push rods. To accurately measure the stress, we use the AD8237 instrumentation amplifier to measure the difference in resistance and amplify it for our ADC to then read. By designing a custom PCB that can accurately measure the stress that certain mechanical components experience we are able to better refine our design.

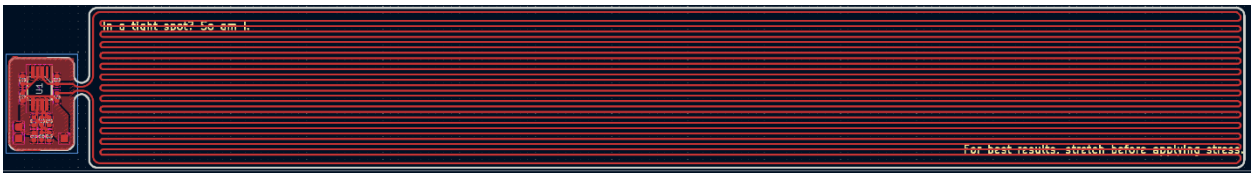


*Figure 106: Strain Gauge Schematic*

# EV Charger

*Figure 107: EV24 Charger Setup*

To charge the accumulator, an off the shelf charger was purchased from EV West. The charger was manufactured by Tesla Motors and supplied the appropriate amount of voltage for our application. The charger was then mounted to a cart with its custom cooling system components, allowing the team to quickly and easily move the setup.

# TSAL

## TSAL Mechanical Design

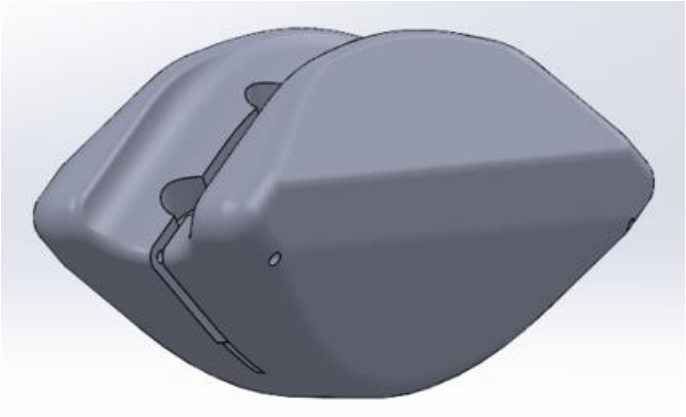

*Figure 108: TSAL Envelope Rev. 1*

In designing the TSAL, a few requirements had to be kept in mind. It had to be made to fit under the highest point of the main roll hoop, it must not be possible for the driver's head to contact the TSAL, and it had to be visible from all (except very small) horizontal angles. To meet these requirements, the TSAL was designed to magnetically connect under the top roll hoop, with holes for zip ties to be sure that it is completely fastened. The housing for the TSAL will be 3D printed in a nearly transparent material, and the PCB will consist of LEDs that can shine through. Originally, the housing was much larger and took up the entire top section of the roll hoop, but after careful consideration the team decided to shrink it down and keep the design sleek. This also helps to ensure that the driver's head will not be able to contact the TSAL. make the TSAL visible from all horizontal angles, the team decided to make the housing convex. Although it does not have to be seen from very small horizontal angles, this will ensure that the TSAL can always be seen and is in compliance with all the rules.

## TSAL Board

The TSAL board contains the 555 timer circuit to control the TSAL lamp as well as the 400 to 24 volt converter. The board has connectors for Vbus+ and Vbus- that are spaced apart for electrical safety.

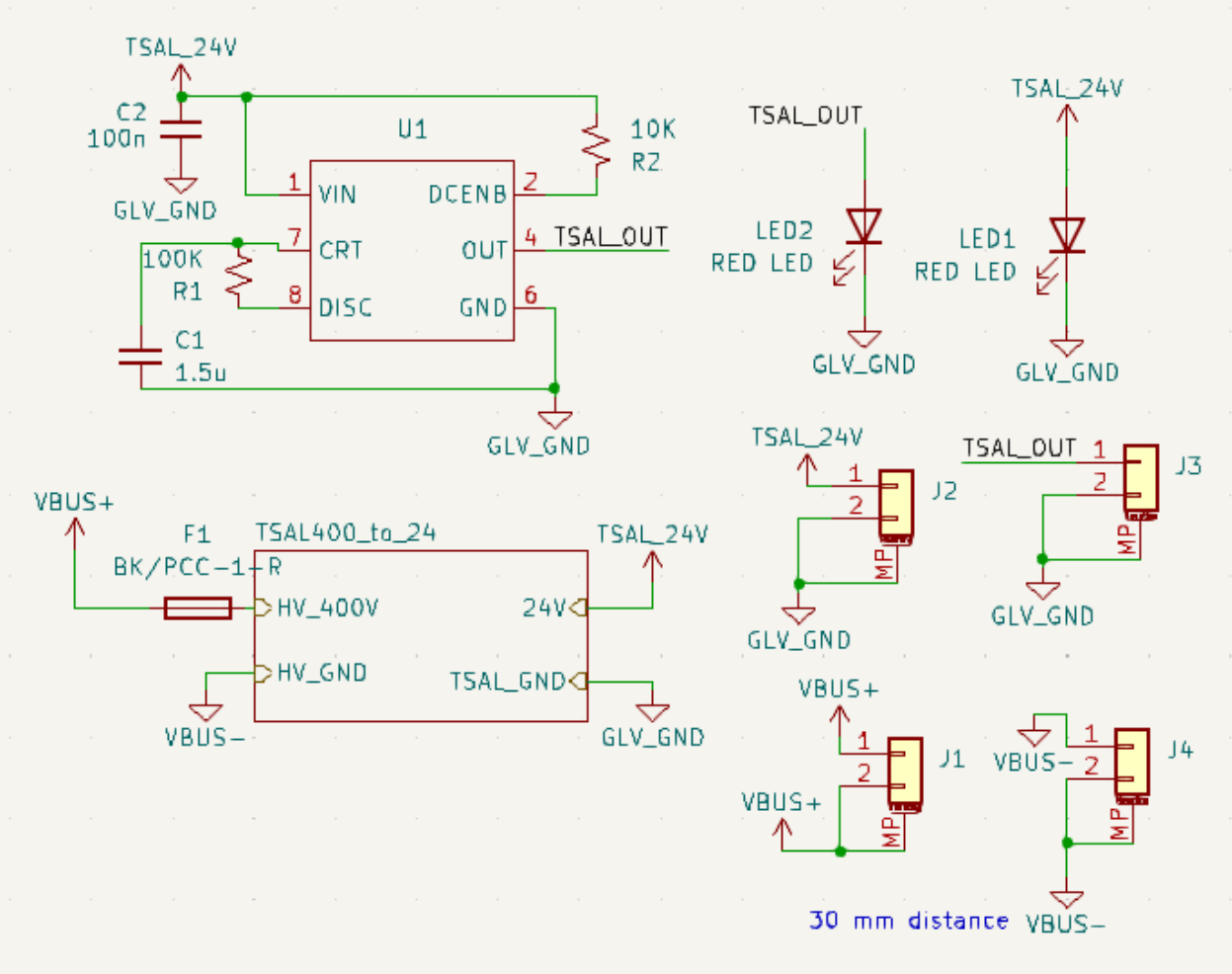


*Figure 109: TSAL Board Schematic Overview*

The isolated 400 to 24 volt converter is connected to the 555 timer for the TSAL Light on the low voltage side. It has connectors for the output of the 555 and for the regular 24 volts. A 555 timer that's compatible with higher voltages was found and used to avoid needing a linear regulator from 24 volts to 12.

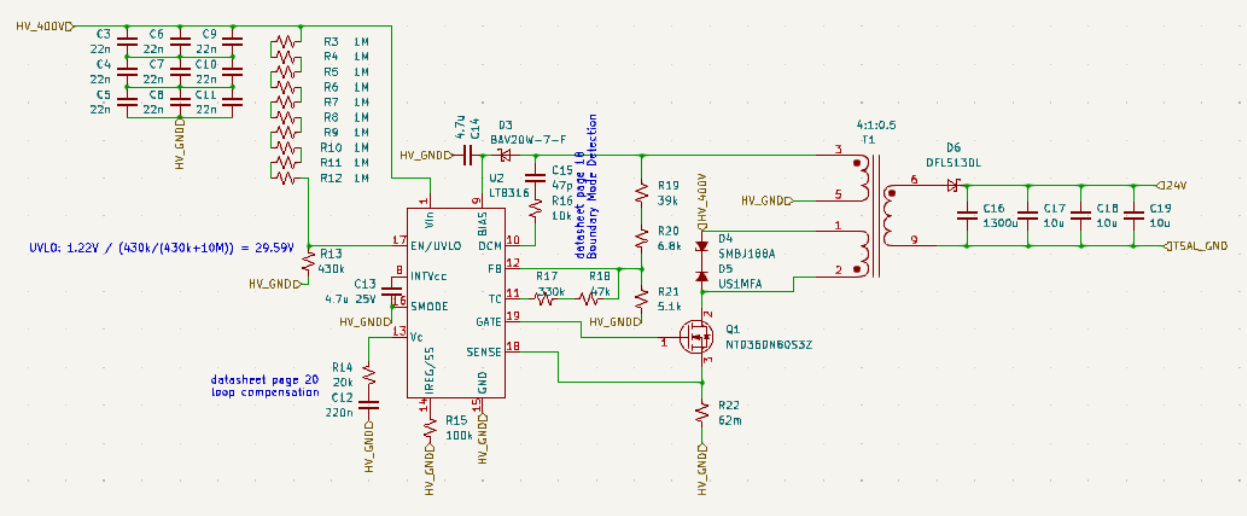


*Figure 110: TSAL Board Schematic Overview Continued*

The layout for this board is roughly 2.2 x 2.4 in. the design is compact while making sure the electrical safety requirements are met. Vbus+ and Vbus- connectors are spaced far apart for safety. There is also an electrical isolation barrier across the board running through the transformer, to separate high and low voltage sides.

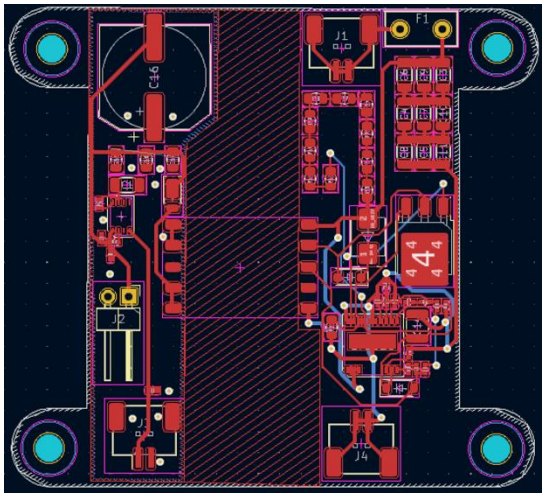

*Figure 111: TSAL Board Schematic*

# Shutdown Control

Mounting components of the high voltage disconnect (HVD), reset buttons, tractive systems measuring point (TSMP), and big red button (BRB) were designed. Two separate waterjet plates on each side of the roll hoop will house the components, each plate will have a 3D printed plastic housing attached by epoxy to the plates and the inward facing side of the box will house an O-ring groove which will mate against a lid. This will ensure no water or other foreign debris enters the box and disrupts the HV and GLV electrical components. The bolted lid will also allow access into the boxes to reach electrical components. The right-side plate incorporates two waterjet steel parts that will house cable glands for the large diameter shielded wires connecting to the HVD.

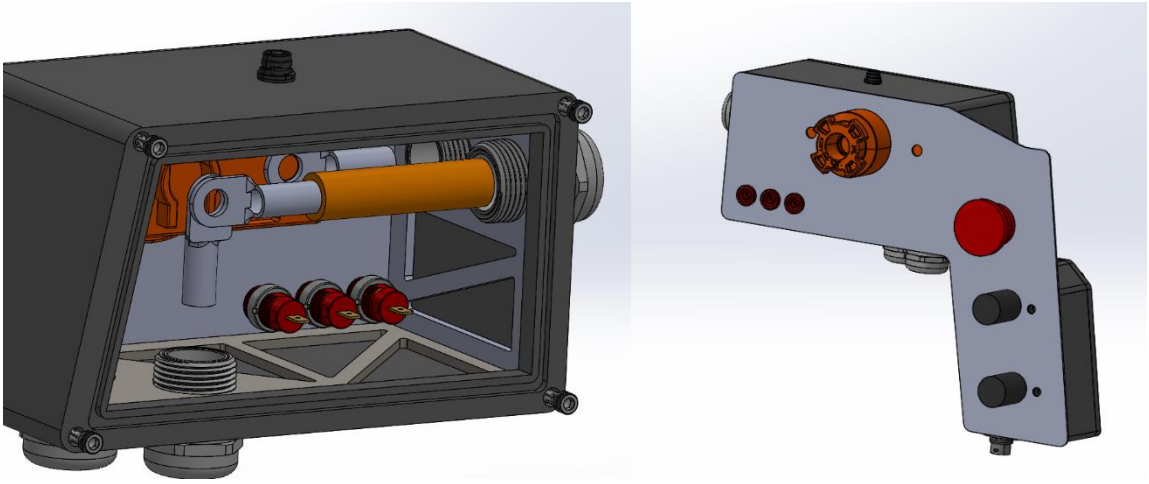

*Figure 112: Right Side Shutdown Control Assembly*

# Conclusions & Recommendations

Our vehicle is highly performant and allows a range of drivers to operate it legally, safely, and comfortably. We are confident that we will produce a strong showing at this year's competition. With that in mind, there are aspects of our vehicle that would benefit from further design iteration. Chief among these is the driver UI/UX - members of the team worked hard to create a design and begin to implement a Formula-style steering wheel, but the full potential of this component has not been reached.


*Figure 113: Steering Wheel Render*

In future years we anticipate this framework will allow drivers to make adjustments and communicate with the team on the fly, furthering our competitive edge. Continuing in that vein, we worked hard to integrate extensive suspension adjustability that future teams will be able to leverage to fine-tune our setup.

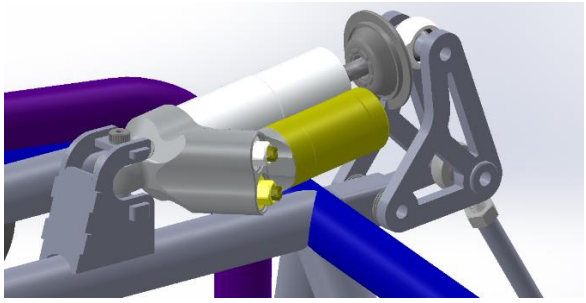

*Figure 114: Suspension Adjustability*

There is also a great deal of room in the competition regulations to further iterate on our aerodynamic package. This year's aerodynamic effort was unprecedented in recent team history, a steppingstone toward better processes and further refined designs. An example of a team pushing the aerodynamic limits of the competition can be seen below.


*Figure 115: Formula Electric + Hybrid Aerodynamic Package Example*

During the Undergraduate Research Project Showcase we also discussed the implementation of a more OEM-style flexible motor mount with multiple judges. Adoption of such a strategy could greatly improve the longevity of our components and frame.

Based on this year's maintenance and implementation experience, the main electrical goals for the coming year include improved segment interchangeability, remote telemetry, and the addition of setup-critical sensing elements such as control arm strain gauges and wheel speed sensors. The groundwork for these concepts have been laid and extensively documented to ensure that future teams will be able to successfully implement our suggestions.

Overall, our hope is that the foundation laid by our team will serve as an effective test bed through which improvements can be made in future years. We worked hard to ensure that our future team members will be able to understand our decisions and learn from our processes as much as possible. Extensive vehicle and driver testing will lead to a highly-tuned machine capable of even better results than this year's competition team.

# Broader Impacts

Our team employed the principles of Engineering Ethics throughout this project. We worked diligently to create both a safe final product and working environment while expanding our engineering competencies. We learned how to professionally engage with intellectual conflict while maintaining perspective on the goal of our project. We also placed a heavy emphasis on working with other engineering departments at WPI to ensure that our lithium-ion cells are stored safely and treated properly at the end of their usable lifecycle. Cell recycling is a crucial topic to the well-being of everyone involved and will play a critical role in the electrification megatrend.

While the economic case for an electric racecar is not straightforward, the landscape of the automotive world is poised to change drastically over the coming years (McKinsey, 2016). Although few people around the world will engage with such a vehicle in their lifetimes, advancing motor vehicle electrification technologies will have an impact on the automotive industry and the world going forward. Decreasing the cost of manufacturing and maintaining electric vehicles will make the market segment more competitive and accessible, ultimately providing more choice to the consumer and decreasing tailpipe emissions.

With those broad impacts established, it is important to note that our design process was heavily influenced by compliance with the relevant competition rules, the full text of which can be found in Appendix IV. Ultimately, the team improved our understanding of how to create accessible, safe, serviceable, and robust systems in a heavily interdisciplinary setting. This unique project has prepared the team to effectively contribute to the ongoing automotive revolution. Moreover, the emphasis on rules compliance and driver safety has improved our ability to produce functional production-ready designs and components across a variety of electro-mechanical applications.

# Works Cited


228 (124kW | 230Nm) - EMRAX. (2024, February 22). EMRAX. https://emrax.com/e-motors/emrax-228/

Automotive revolution – perspective towards 2030. (2016, January 1). McKinsey & Company. https://www.mckinsey.com/industries/automotive-and-assembly/our-insights/disruptive-trends-that-will-transform-the-auto-industry/de-de

Dartmouth Engineering. (2022). FH+E 2022. Formula Hybrid + Electric. https://www.flickr.com/photos/thayerschool/52056419027/in/album-72177720298729343/

Demetriades, Z., Seay, D., & Zogheib, J. (2020). FSAE Zips Electric Racing Brake System Design. University of Akron Department of Mechanical Engineering. https://static1.squarespace.com/static/64a33216a488de2dac5ab824/t/64c864781e3077336843b4b4/1690854525570/Senior+Design+Proposal+for+Brakes+Subsystem+2019-2020.pdf

Documents. (2023). Formula Hybrid + Electric. https://www.formula-hybrid.org/documents

Katz, J. (2006). AERODYNAMICS OF RACE CARS. *Annual Review of Fluid Mechanics*, *38*(1), 27–63. https://doi.org/10.1146/annurev.fluid.38.050304.092016

Katz, J., & Garcia, D. (2002). Aerodynamic effects of Indy car components. *SAE Technical Papers on CD-ROM/SAE Technical Paper Series*. https://doi.org/10.4271/2002-01-3311

keenlab. (2024, April 25). kWeld – complete kit | keenlab. Keenlab | Electronic Projects and Engineering Services. https://www.keenlab.de/index.php/product/kweld-complete-kit/

OGAWA, A., MASHIO, S., NAKAMURA, D., MASUMITSU, Y., MINAGAWA, M., & NAKAI, Y. (2009). *Aerodynamics Analysis of Formula One Vehicles*. https://www.f1-forecast.com/pdf/F1-Files/Honda/F1-SP2_21e.pdf

WPI Formula SAE. (n.d.). WPI Formula SAE -. https://wp.wpi.edu/wpifsae/

# Appendix

## I. 2024 Design Report

2024 Design Report.pdf

## I. WPI EV24 ESF2

WPI EV24 ESF2.pdf

## II. WPI EV24 Change Management Report

204_Worcester Polytechnic Institute_

## III. MQP Project Showcase 2024: Mechanical & Materials Engineering Slideshow

Mech PPD Slideshow.pdf

## IV. Competition Rules Documents

2024 Formula Hybrid+Electric Rules

## V. Brake System Calculations

Brake Calculations.pdf